CLONING AND EXPRESSION PROFILE OF *FLT3* GENE DURING RAT LIVER REGENERATION

A THESIS SUBMITTED TO
THE DEPARTMENT OF MOLECULAR BIOLOGY AND GENETICS
AND THE INSTITUTE OF ENGINEERING AND SCIENCE OF
BILKENT UNIVERSITY
IN PARTIAL FULFILLMENT OF THE REQUIREMENTS
FOR THE DEGREE OF MASTER OF SCIENCE

BY
IRAZ TOPRAK AYDIN
AUGUST 2005

I certify that I have read this thesis and that in my opinion it is fully adequate, in scope and in quality, as a thesis for the degree of Master of Science.

Assist. Prof. Dr. Can Akçalı

I certify that I have read this thesis and that in my opinion it is fully adequate, in scope and in quality, as a thesis for the degree of Master of Science.

Assist. Prof. Dr. Özlen Konu

I certify that I have read this thesis and that in my opinion it is fully adequate, in scope and in quality, as a thesis for the degree of Master of Science.

Prof. Dr. Alp Can

Approved for the Institute of Engineering and Science:

Prof. Dr. Mehmet B. Baray
Director of the Institute Engineering and Science

ABSTRACT

CLONING AND EXPRESSION PROFILE OF *FLT3* GENE DURING RAT LIVER REGENERATION

Iraz Toprak Aydın
M.S. in Molecular Biology and Genetics
Supervisor: Assist. Prof. Dr. Can Akçalı
August 2005, 73 Pages

Liver has a unique capacity to regenerate itself upon exposure to viral infections, toxic reactions and cancer formation which result in the loss of hepatocyte. Liver regeneration is a complex phenomenon in which several factors participate during its onset. Cellular proliferation is one of the important component of this process and the factors regulate this proliferation has a vital role. FLT3, a well-known hematopoietic stem cell and hepatic lineage surface marker, takes place in proliferative events of hematopoietic stem cells. However, its contribution to liver regeneration is not known. Therefore, in this study, we aimed to examine the role of FLT3 during liver regeneration. First we cloned a partial cDNA of rat homolog of FLT3 from thymus and examined the tissue specific expressions both in mRNA and protein level. After performing hepatectomy in rats to induce liver regeneration, expression profile of FLT3 in both mRNA and protein level and its cellular localization were also investigated during the different stages of liver regeneration models. Our data showed that FLT3 is expressed in most of the rat tissues and in liver regeneration. However, its intracellular localization is changed during the late stages of liver regeneration. Therefore, our results suggest a mechanism in which FLT3 receptor is activated in the late stages of liver regeneration.

Keywords: liver regeneration, FLT3, oval cells, rat.

ÖZET

SIÇAN *FLT3* GENİNİN KLONLANMASI VE SIÇANLARDA KARACİĞER REJENERASYONUNDA *FLT3* GENİNİN İFADE PROFİLİNİN İNCELENMESİ

Iraz Toprak Aydın
Moleküler Biyoloji ve Genetik, Yüksek Lisans
Tez Yöneticisi: Yard. Doç. Dr. Can Akçalı
Ağustos 2005, 73 Sayfa

Karaciğerin viral enfeksiyonlar, toksik reaksiyonlar ve kanser oluşumu sonucu meydana gelen hepatosit kaybı karşısında, özel bir rejenerasyon kapasitesi vardr. Karaciğer rejenerasyonu, birçok faktörün katılımı ile gerçekleşen karmaşık bir olaydır. Hücresel proliferasyon bu sürecin önemli parçalarından biri olduğundan, proliferasyonu düzenleyen etkenlerin rejenerasyonda önemli bir rolü vardır. Hematopoetik kök hücre ve hepatik-kökenli hücre işaretleyicisi olarak bilinen FLT3 proteininin hematopoetik kök hücrelerde proliferasyonda görev aldığı kabul edilmektedir. Ancak karaciğer rejenerasyonunda katkısı bilinmemektedir. Bu yüzden, bu çalışmada FLT3'ün karaciğer rejenerasyonundaki rolünü araştırmayı amaçladık. Öncelikle sıçan timusundan FLT3 homoloğunun kısmi cDNAsını klonlayarak FLT3'n değişik dokularda ifadesini mRNA ve protein düzeyinde inceledik. Sıçanlarda kısmi karaciğer çıkarılması ile oluşturduğumuz karaciğer rejenerasyon modellerinin değişik aşamalarında FLT3'ün mRNA ve protein düzeyinde ifade profilini ve hücresel lokalizasyonunu araştırdık. Elde ettiğimiz veriler FLT3'ün birçok sıçan dokusunda ve karaciğer rejenerasyonu sürecinde ifade edildiğini göstermektedir. Bununla birlikte rejenerasyonun ileri aşamalarında, FLT3'ün hücre içi lokalizasyonunda bir farklılık olduğunu saptadık. Sonuçlarımız, FLT3 reseptörünün karaciğer rejenerasyonun ileri aşamalarında aktif hale geldiğini düşündürtmektedir.

Anahtar sözcükler: karaciğer rejenerasyonu, FLT3, oval hücreler, sıçan.

Acknowledgement

I'd like to express my gratitude to...

...my supervisor Assist. Prof. Can Akçalı, for his valuable supervision, precious guidance, unending support, patience and encouragement during this study,

...Assist. Prof. Özlen Konu, for her incredible support during my studies, and for joining my thesis defense committee,

...Assoc. Prof. Aydın Dalgıç, for helping us with the PH and SH operations in the middle of night, after a hard day's work of life saving,

...Bala Gür and Nuri Öztürk, for their help, for their incredible patience for my endless questions, and of course for their friendship,

...Ceren Sucularlı, for her unconditional friendship,

...Pınar Özdemir, Şerif Şentürk, Ece Terzioğlu, Fatma Ayaloğlu, Ayça Ergül, Elif Uz, and all Bilkent MBG family members, for their friendship, help and support during those two years,

...Ayşegül Altın and Çiğdem Sevim; for being the best flatmates I have ever had and probably I will ever have, for being there for me, and for making life in Ankara bearable for me,

...other members of ITUMBG quartet (Burcu, Şirin, Hande) and Canan, Meltem, Ayşe, Nilay, Gizem, Behire and all 6-FEN-A gang, for their loyal friendship over all those years,

...my mentor, Assoc. Prof. Benan Dinçtürk; for giving me the wings, for pushing me off the nest and for believing in me,

...and last, but not least, my family, especially my mother, my sister and my aunt for their unconditional love and for their unlimited support for all my decisions...

Table of Contents

List of Tables

List of Figures

Abbreviations

4E-BP1	4E-Binding Protein
AAF	2-acetylaminofluorene
BAD	BCL2 antagonist of cell death
β-ME	β-Mercaptoethanol
BFB	Bromophenol Blue
BSA	Bovine Serum Albumin
CBB	Coomassie Brilliant Blue G-250
cDNA	complementary Deoxyribonucleic Acid
C/EBPα	CCAAT/enhancer binding protein-α
CREB	Cyclic Adenosine Monophosphate-Response Element Binding Protein
C_t	Cycle Treshold
CYC	Cyclophilin
ddH_2	Deionized Water
DEN	Diethylnitrosamine
DEPC	Diethylpyrocarbonate
dH_2O	Distilled Water
DNA	Deoxyribonucleic Acid
DNase	Deoxyribonuclease
EGF	Epidermal Growth Factor
ERK	Extracellular-Signal-Regulated Kinase
FAH	Fumarylacetoacetate Hydrolase
FLT3L	FLT3 Ligand
FLK2	Fetal Liver Kinase 2
FLT3	FMS-Like Tyrosine Kinase 3
FLT3L	FLT3 Ligand
FMS	Macrophage Colony-Stimulating Factor Receptor
GAB2	GRB2-Binding Protein
HSC	Hematopoietic Stem Cells
HGF	Hepatocyte Growth Factor

HRP	Horseradish Peroxidase
IHC	Immunohistochemistry
IL-6	Interleukin-6
lt	liter
M	Molar
μg	Microgram
μl	Microliter
MEK	MAPK/ERK kinase
mg	Milligram
ml	Milliliter
mM	Millimolar
mTOR	Mammalian Target Of Rapamycin
NL	Normal Liver
OD	Optical Density
PAGE	Polyacrylamide Gel Elecrophoresis
PBS	Phosphate Buffered Saline
PCR	Polymerase Chain Reaction
PDK1	3-Phosphoinositide-Dependent Protein Kinase 1
PFA	Paraformaldehyde
PH	Partial Hepatectomy
PI3K	Phosphatidylinositol 3-Kinase
PKB	protein kinase B
RNA	Ribonucleic Acid
RNase	Ribonuclease
RT-PCR	Reverse-Transcriptase Polymerase Chain Reaction
RTK	Receptor Tyrosine Kinase
S6K	S6 kinase
SDS	Sodium Dodecyl Sulfate
SH	Sham Operation
SHC	SH2-Containing Sequence Protein
SHIP	SH2-Domain-Containing Inositol Phosphatase

SHP2	SH2-Domain-Containing Protein Tyrosine Phosphatase 2
STAT	Signal Transducer and Activators of Transcription
STK-1	Stem Cell Tyrosine Kinase 1
TGFα	Transforming Growth Factor-α
TGFβ1	Transforming Growth Factor-β 1
TKD	Tyrosine Kinase Domain
T_m	Melting Temperature
TNFα	Tumor Necrosis Factor-α
XC	Xylene Cyanole

Chapter 1

Introduction

1.1 Liver

The liver is the largest mass of glandular tissue in mammalian body. It is located in the upper right quadrant of the abdominal cavity. It receives a supply of arterial blood from hepatic arteries, and from veins of the digestive tube, pancreas and spleen via the hepatic portal vein. Thus, the liver stands directly in the pathway of blood vessels that bring substances absorbed from the digestive tube. This position gives the liver the first chance to metabolize these substances. It also makes it the first organ to be exposed to toxic compounds that have been ingested. (Ross *et al*, 1989)

The liver serves several metabolic functions. Some of these functions are: (Simpkins and Williams, 1998; Carola *et al*, 1992)

- formation of urea from amino acids
- manufacture of blood proteins
- formation of erythrocytes during fetal life
- synthesis of the blood-clotting agent fibrinogen

- detoxification of many poisons
- synthesis of bile and bile salts for emulsification of fats in the small intestine.

1.1.1 Origin of Mammalian Liver

At the 12-25 somite stage, the liver emerges from the definitive gut endoderm first as a thickening of the ventral endodermal epithelium and then as a bud of cells that proliferate and migrate into the surrounding septum transversum mesenchyme (Figure 1.1 A, B). The nascent hepatocytes surround spaces within the septum transversum mesenchyme and the entire domain becomes delineated or encapsulated as the liver bud grows rapidly into an organ (Figure 1.1 C). The general architecture of the liver is laid down at this point (Zaret, 2000; Gilbert, 2003).

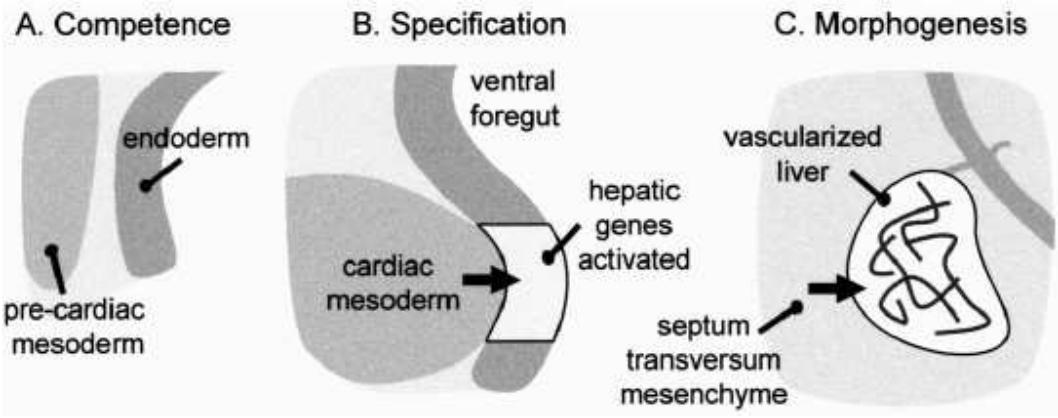

Figure 1.1: *Overview of Early Liver Development (Zaret, 2000)*

During fetal life, the liver is the main site of hematopoiesis and up to 60% of the liver mass consists of blood cells (Paul *et al*, 1969). During the perinatal period, a large number of metabolic enzymes are induced within the hepatocytes as the hematopoietic cells migrate elsewhere and the liver prepares to control metabolite and serum protein levels in the blood, store glycogen, and detoxify (Zaret, 2000).

1.1.2 Organization of Mammalian Liver

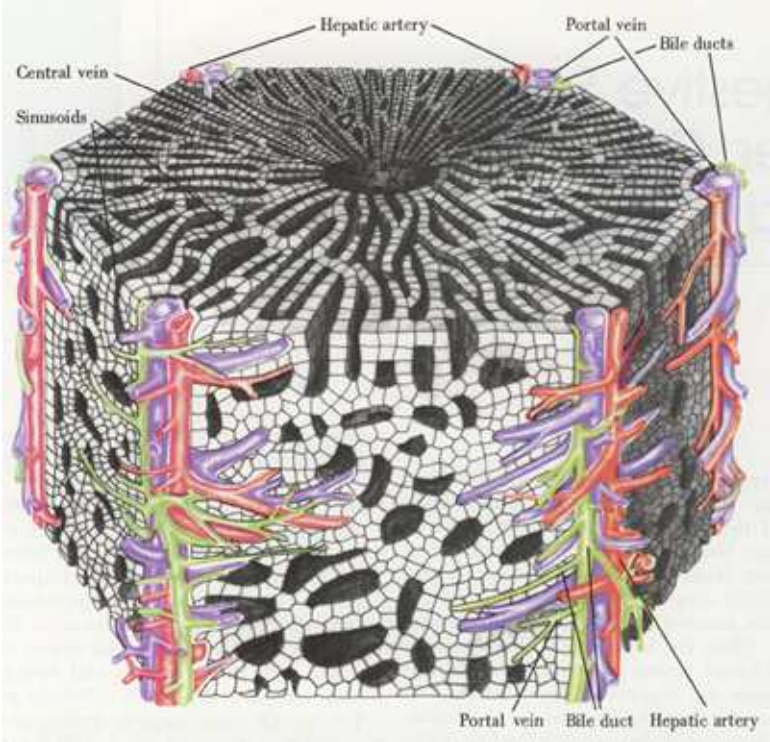

Figure 1.2: *The Histological Structure of the Liver Lobule (Ross* et al*, 1989)*

The liver is divided into four lobes. The site where the portal vein, hepatic artery, bile duct, nerves, and lymphatic vessels enter/leave the liver is called port hepatis. The portal vein, hepatic artery, and bile duct course together as a triad, called portal triad, through the stromal ramifications of the liver. The main cell types resident in the liver are hepatocytes, bile duct epithelium, stellate cells, Kupffer cells, vascular endothelium, fibroblasts, and leukocytes (Guyton and Hall, 1996; Lanza *et al*, 2004; Ross *et al*, 1989).

The structural and functional unit of the liver is the liver lobule (Figure 1.2). The central structure of the lobule, traversing its long axis, is the central vein. Plates of hepatocytes radiate from central vein to the perimeter of the lobule. The plates are one cell thick and are separated by the hepatic sinusoids, which are also radially arranged about the central vein. The angular space that contains the portal triad and the surrounding connective tissue is called the portal canal.

This canal is bordered by the outer most hepatocytes of the lobule (Guyton and Hall, 1996; Lanza *et al*, 2004; Ross *et al*, 1989).

Bile secreted by hepatocytes is collected in bile ducts, lined by duct epithelial cells. The canal of Hering is the connection between the bile canaliculi and the bile ducts at the interface between the lobule and the portal triad (Guyton and Hall, 1996; Lanza *et al*, 2004; Ross *et al*, 1989).

1.2 Liver Regeneration

Liver not only provides means for the body, but also has a great capacity to regenerate upon harmful conditions with a process known as liver regeneration as illustrated by the ancient Greek legend of Prometheus. In experimental conditions, it has been shown that animals can survive surgical removal of up to 75% of the total liver mass (Bucher and Swaffield, 1964).

There are three separate mechanisms for liver regeneration (Grompe and Finegold, 2001):

1. normal tissue turnover
2. hepatocyte-driven regeneration after liver injury
3. progenitor-dependent regeneration after liver injury

1.2.1 Liver Regeneration During Normal Tissue Turnover

The average life span of adult mammalian hepatocytes has been estimated to be ∼200-300 days. One of the models regarding normal liver turnover was called the streaming liver. According to this model, normal liver turnover is similar to regeneration in the intestine. In this model, young hepatocytes born in the

portal zone migrate toward the central vein. The gene expression patterns of the hepatocytes, that were located at different zones of the liver, were different. This phenomenon was explained by the aging process during the migration, which represented a typical lineage progression. It is also explained that the ploidy and size of hepatocytes depend on their location within the lobule (Zajicek *et al*, 1985, Arber *et al*, 1988). Central hepatocytes tend to be larger and more polyploid than periportal hepatocytes. However, other studies provided strong evidence against the streaming liver model. First, it was shown that the difference in gene expression pattern in hepatocytes was dependent on the direction of blood flow (Thurman and Kauffman, 1985). If blood flow was reversed such that portal blood entered the lobule through the central vein and exited via the portal vein, the pattern inverted. Therefore, the lobular zonation is best explained by metabolite-induced gene regulation, not lineage progression. Second, retroviral marking studies provide evidence against any hepatocyte migration during normal turnover (Bralet *et al*, 1994; Kennedy *et al*, 1995). Retrovirally marked hepatocytes formed small clones that remained largely coherent and were equally distributed in all zones of the liver. These results were confirmed in studies utilizing the mosaic pattern of X-inactivation in female mice to analyze patterns of hepatocyte growth (Shiojiri *et al*, 1997, 2000). Thus, current evidence suggests that normal liver turnover in adult animals is mediated primarily by *in situ* cell division of hepatocytes themselves and not stem cells (Ponder, 1996).

1.2.2 Regeneration After Partial Hepatectomy (PH)

During PH, specific lobes of liver are removed intact without damage to the lobes left behind. The residual lobes grow to compensate for the mass of the resected lobes, although the removed lobes do not grow back. The process is completed within one week. There is no evidence for involvement or requirement of stem cells during this process. Thymidine labeling studies show that virtually all hepatocytes in the remaining liver divide once or twice to restore the original cell number within 3-4 days (Bucher and Swaffield, 1964).

As shown in figure 1.3 the earliest hepatocytes are seen 24 hours after PH. There is zonal variation depending on how much tissue is removed. When only 15% of the liver is surgically removed, periportal hepatocytes divide preferentially where as cell division is seen equally in all zones of liver after 75% PH. Following the hepatocytes, other hepatic cell types also undergo a wave of mitosis, thereby restoring the original number of cells within 7 days (Bucher and Swaffield, 1964; Michalopoulus and DeFrances, 1997).

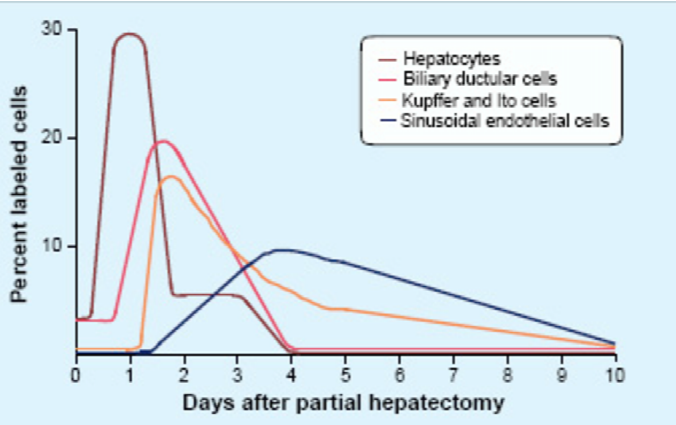

Figure 1.3: *Time Course of Liver Regeneration (Michalopoulus and DeFrances, 1997)*

1.2.2.1 Factors Involved in Regeneration After PH

Several factors are involved in induction of hepatocyte cell division. HGF is a primary mitogen for hepatocytes and is responsible for the early events after PH. The earliest event that takes place within one minute after PH, is a large increase in the blood level of HGF (Lindroos *et al*, 1991). It is thought that PH causes remodeling of extracellular matrix in the liver and release of HGF stored there. HGF then binds to its receptor c-met and activates a signal transduction pathway leading to re-entry of hepatocytes into the cell cycle (Bottaro *et al*, 1991).

Other cytokine-receptor interactions are also important in the cascade resulting in mitosis. Known factors are IL-6, TNFα, TGFα, and EGF. Deficiency

of IL-6 and TNFα in mice caused delayed regeneration after PH (Cressman *et al*, 1996; Taub, 1996; Yamada *et al*, 1997; Yamada and Fausto, 1998). EGF is a primary mitogen for hepatocytes in tissue culture (Michalopoulos *et al*, 1984; Lindroos *et al*, 1991), but its role in liver regeneration *in vivo* is not clear since EGF levels increase only a little after PH (Noguchi *et al*, 1991). In contrast, it is shown that, TGFα mRNA and protein levels show an important increase within hours after PH (Mead and Fausto, 1989), and TGFα overexpression can drive hepatocyte replication *in vivo*.

Non-peptide hormones also have an important role in the regeneration after liver injury. Triiodothyronine (Short *et al*, 1980) and norepinephrine (Cruise *et al*, 1988; Cruise, 1991) can stimulate hepatocyte replication *in vivo*. The relationship of these factors with progenitor-dependent liver regeneration or engraftment as well as expansion of liver stem cells, is not known (Grompe and Finegold, 2001).

The mechanisms by which hepatocyte cell division and liver regeneration cease after the appropriate liver mass has been restored is not clearly known. In particular, the exogenous signals (endocrine, paracrine, or autocrine) involved in sensing the overall liver cell mass and negatively regulating its size are not known. Some studies suggests that TGFβ1 may be important in terminating liver regeneration (Jirtle *et al*, 1991). Some endogenous signals are known to participate in the negative regulation of hepatocyte growth. They include general tumor suppressor genes. Mice lacking p53 or the p53-inducible cell cycle regulatory protein p21 have been shown to have continuous hepatocyte turnover (Wu *et al*, 1996; Yin *et al*, 1998). Some other hepatocyte-specific transcription factors, like C/EBPα, are also known to play a role in liver regeneration (Wang et al. 1995; Timchenko et al. 1996).

1.2.3 Progenitor Cell-Dependent Liver Regeneration

When liver damage is so severe that hepatocytes are largely killed or that their proliferation is prevented by exposure to hepatotoxins or carcinogens, liver progenitor cells with a high nuclear/cytoplasmic ratio, appear in the periportal areas of liver lobules. These small-cells proliferate extensively, and migrate into the lobule. These cells, which then become differentiated hepatocytes, are called oval cells because of their initial morphology (Shinozuka *et al*, 1978). Oval cells are thought to have the ability to proliferate clonogenically and a bipotential capacity to differentiate into both hepatocytes and bile duct cells and have lineage options similar to those displayed by hepatoblasts in early stages of liver development (Vessey and de la Hall, 2001; Kruglov *et al*, 2002; Sirica *et al*, 1990; Sirica, 1995).

The oval cells initially appear next to biliary ductules and then some migrate into the hepatic parenchyma. It has recently been shown that mesenchymal stem cells can differentiate into hepatocytes passing through oval cell stage (Hong *et al*, 2005). Oval cell precursors located in the canal of Hering represent likely candidates for liver-repopulating stem cells, and can be considered a facultative liver stem cell (Fausto *et al*, 1993; Theise *et al*, 1999). It also has been shown that oval cells first change into basophilic small hepatocytes and then differentiate into mature hepatocytes (Mitaka, 2001).

Oval cell proliferation represents progenitor cell-dependent liver regeneration. In progenitor-dependent liver regeneration, the hepatocytes themselves cannot divide normally. Thus, progenitor-dependent liver regeneration is utilized when parenchymal hepatocytes are severely damaged on a chronic basis and unable to regenerate efficiently (Fausto *et al*, 1993; Theise *et al*, 1999). Progenitor-cell dependent liver regeneration can be triggered by different methods (Table 1.1).

Chemical/Manipulation	**Reference**
AAF	Teebor and Becker, 1971
DEN	Schwarze *et al*, 1984
DEN + AAF + PH	Solt *et al*, 1977
AAF + PH	Evarts *et al*, 1990
Choline-deficient diet + DL-ethionine	Shinozuka *et al*, 1978
D-Galactosamine + PH	Lemire *et al*, 1991
Lasiocarpine + PH	Laconi *et al*, 1995
Retrorsine +PH	Laconi *et al*, 1998; Gordon *et al*, 2000

Table 1.1: *Induction of Progenitor-Dependent Liver Regeneration in Rat (Grompe and Finegold, 2001)*

To induce oval cells in the rat liver, the combination of 2-acetylaminofluorene (AAF) treatment and PH is often used. AAF is metabolized to its cytotoxic and mitoinhibitory N-hydroxy derivative molecule by the phase I metabolic enzymes, which are strongly expressed specifically in adult hepatocytes but relatively low expressed in biliary cells and oval cells (Alison *et al*, 1998). The continuous administration of a low concentration of AAF suppress the proliferation of hepatocytes and at the middle point of the treatment the animals are subjected to a massive loss of hepatocytes by PH. When the hepatocytes do not respond to growth signals, this results in the rapid growth of oval cells (Mitaka, 2001).

Oval cells express both hepatic markers and hematopoietic stem cell markers such as albumin, AFP, Thy-1, FLT3, c-KIT, CK-18, and CK-19 (Grompe and Finegold, 2001).

1.3 FLT3: An Oval Cell Marker

The *FLT3* (*FLK2, STK-1*) gene encodes a membrane bound RTK (Stirewalt and Radich, 2003). The mouse *FLT3* gene was cloned by two independent groups in 1991 (Matthews *et al*, 1991; Rosnet *et al*, 1991). The human *FLT3* gene was, cloned in 1993 (Rosnet *et al*, 1993) whereas rat homolog of FLT3 cDNA has not been cloned.

1.3.1 Structure of FLT3

FLT3 encodes an RTK of 993 amino acids in length that belongs to the RTK subclass III family. FLT3 receptor is a membrane-bound receptor (Figure 1.4) with five immunoglobulin-like extracellular domains, a transmembrane domain, a juxtamembrane domain and two intracellular TKDs linked by a kinase-insert domain (Agnes *et al* 1994; Stirewalt and Radich, 2003).

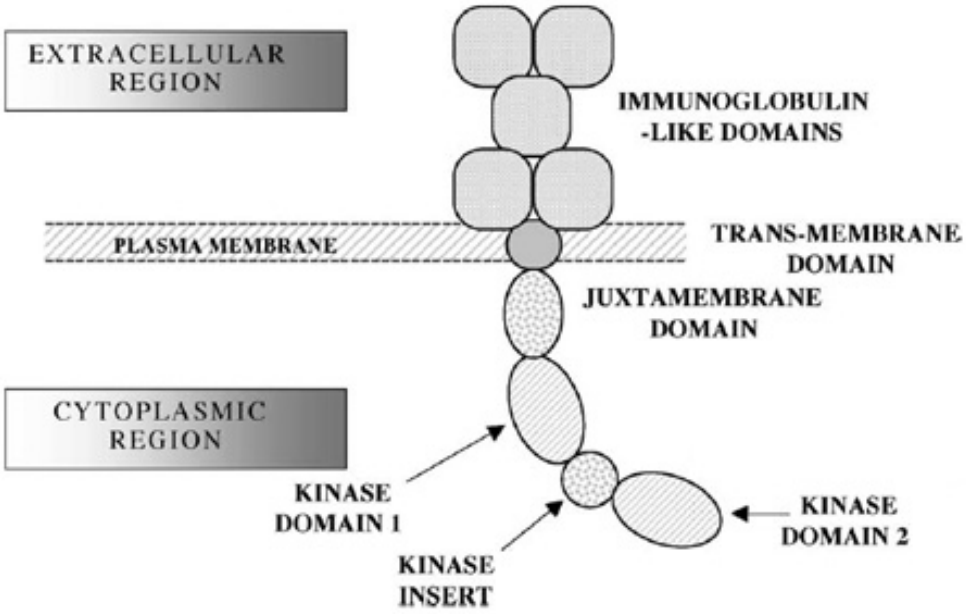

Figure 1.4: *Structure of FLT3 Receptor (Markovic* et al*, 2005)*

1.3.2 Activation of FLT3

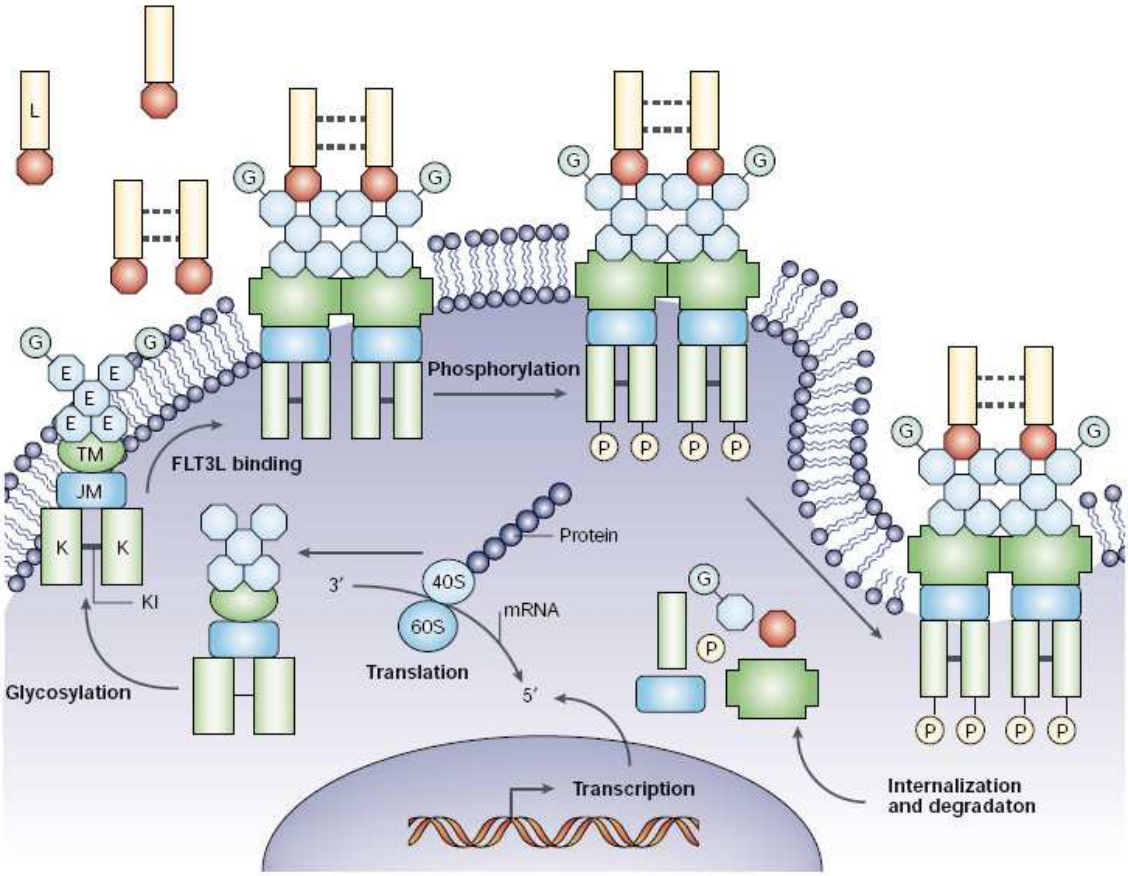

Figure 1.5: *Activation of FLT3 Receptor (Stirewalt and Radich, 2003)*

Unstimulated FLT3 receptors are in monomeric form in the plasma membrane (Figure 1.5). In this inactive state, the conformation of the receptor might result in steric inhibition of dimerization and exposure of phosphoryl acceptor sites in the TKD by the juxtamembrane domain (Stirewalt and Radich, 2003). After stimulation with the ligand, FLT3L, membrane-bound FLT3 quickly changes conformation, and forms a homodimer and exposes phosphoryl acceptor sites in TKD (Turner *et al*, 1996). Dimerization stabilizes this conformational change which further enhances activation of the receptor (Weiss and Schlessinger, 1998).

Phosphorylation of FLT3 occurs within 5-15 minutes after FLT3L binding. The FLT3L-FLT3-phosphate complex is then rapidly internalized, starting within

5 minutes of stimulation and reaching a maximum after 15 minutes. Degraded byproducts of ligand-receptor complex are seen as early as 20 minutes after stimulation (Turner *et al*, 1996).

The entire process of activation, internalization and degradation of FLT3 occurs rapidly in cells. The rate of FLT3 production, the speed of degradation of the activated FLT3L-FLT3 complex, and the downstream effects of activation probably participate in a complex feedback loop that regulates normal receptor activity (Stirewalt and Radich, 2003).

1.3.3 The FLT3 Signal Transduction Pathway

Binding of FLT3L to FLT3 triggers the PI3K and RAS pathways (Figure 1.6), which lead to increased cell proliferation and the inhibition of apoptosis. PI3K activity is regulated through various interactions between FLT3, SHCs and one or more other proteins, such as SHIP, SHP2, CBL and GAB2. Activated PI3K stimulates downstream proteins such as PDK1, PKB (AKT) and mTOR, which initiate the transcription and translation of crucial regulatory genes through the activation of p70 S6K and the inhibition of eukaryotic initiation factor 4E-BP1. In addition, PI3K activation blocks apoptosis through phosphorylation of the pro-apoptotic BCL2-family protein BAD. Activated FLT3 also associates with GRB2 through SHC, so activating RAS. RAS activation stimulates downstream effectors such as RAF, MEKs, ERK, and the 90-kDa ribosomal protein S6 kinase. These downstream effectors activate CREB, ELK and STATs, which lead to the transcription of genes involved in proliferation. Both pathways probably also interact with many other antiapoptotic and cell-cycle proteins, such as WAF1, KIP1 and BRCA1 (Stirewalt and Radich, 2003).

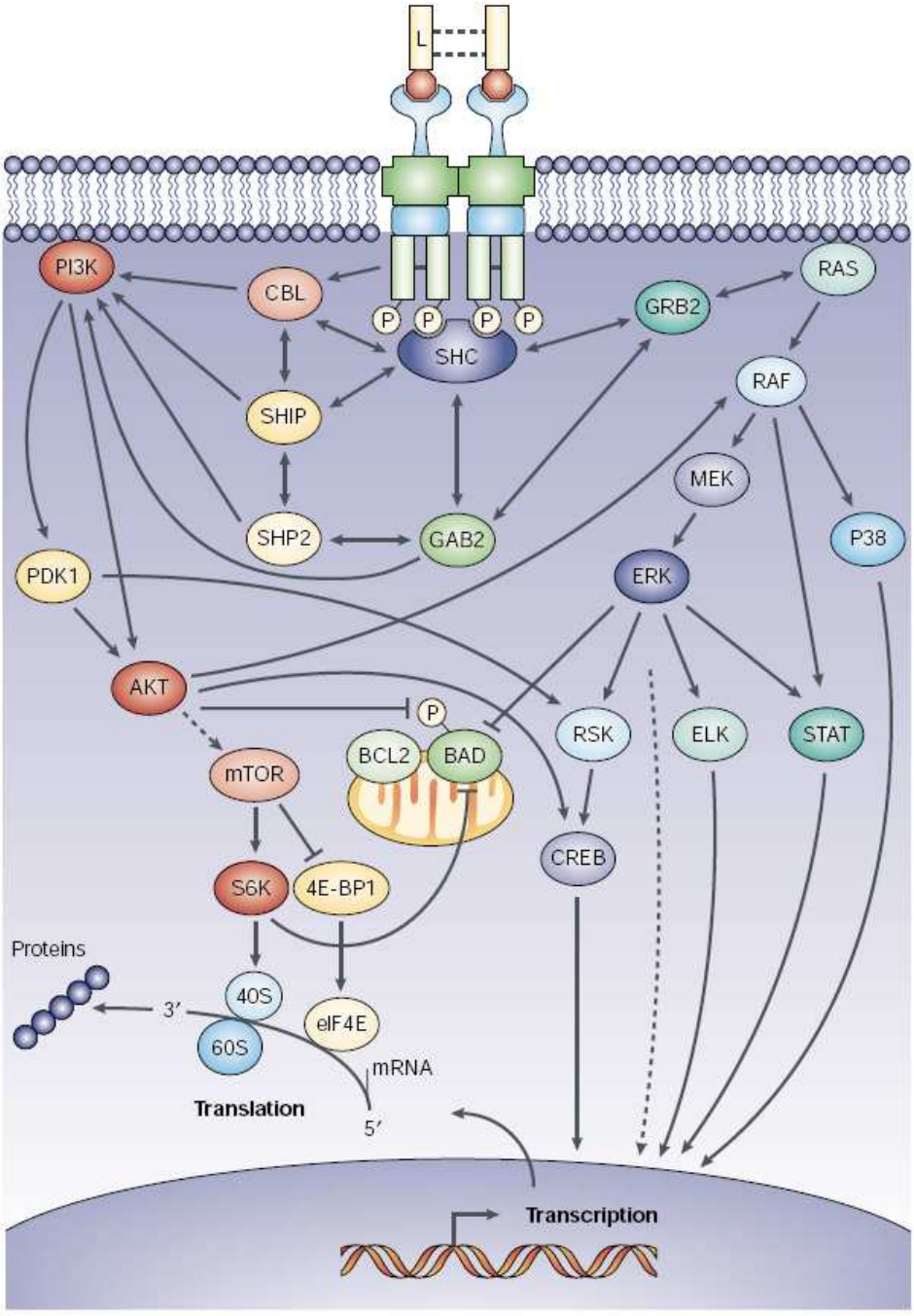

Figure 1.6: *The FLT3 Signaling Cascade (Stirewalt and Radich, 2003)*

Chapter 2

Aim of the Study

2.1 Aim

Liver responds to certain toxic viral agents or to any condition that results in the loss of hepatocytes by undergoing regeneration. One of the specific feature of regenerating liver is an induction in the oval cell population, characterized by the expression of FLT3 among with other factors.

FLT3 is a well-known hematopoietic stem cell marker that plays a role in proliferative events. Recent studies support that FLT3 also is a hepatic lineage surface marker (Hong *et al*, 2005). Its existence in oval cells further support its crucial role in hepatocyte development. However, the expression pattern of FLT3 during liver regeneration has not been investigated.

In this study our aim was, first to clone and monitor the tissue specific expression of rat homolog of *FLT3* gene. We also aimed to show the changes in the expression of FLT3 in both mRNA and protein level, in two models of liver regeneration, namely hepatocyte-driven liver regeneration and progenitor cell-dependent liver regeneration.

2.2 Strategy

In order to achieve the cloning of rat homolog of *FLT3* gene, we decided to amplify the coding region of the gene in three overlapping fragments. For the amplification of fragments, total cDNA from rat thymus was used as template.

After cloning, we investigated the pattern of FLT3 expression at both mRNA and protein level in different rat tissues.

Two types of liver regeneration; regeneration after PH and progenitor cell-dependent liver regeneration, were used as models in this study. For the first model, PH and SH operations were performed. For the second model, progenitor cell-dependent regeneration was induced by the administration of AAF followed by PH or SH operations.

Liver samples were collected from rats at certain times throughout the course of regeneration. FLT3 expression at both mRNA and protein level was measured for all groups. Expression at mRNA level was detected by semi-quantitative PCR and real-time PCR. Protein expression was detected by western blotting. The localization of FLT3 protein was observed by IHC.

Chapter 3

Materials and Methods

3.1 Animals

Male, 9-weeks old and 200-300 grams Sprague-Dawley rats were used. They were housed under controlled environmental conditions (22°C) with a 12-hour light and 12 hour dark cycle in the animal holding facility of the Department of Molecular Biology and Genetics at the Bilkent University, Turkey. The animals were permitted unlimited access to food and water at all times.

3.2 Solutions and Buffers

PBS

Stock solution (10XPBS) was prepared by dissolving 80g NaCl, 2g KCl, 11.5g $Na_2HPO_4.7H_2O$, and 2g KH_2PO_4 in 1lt ddH_2O. Working solution (1XPBS) was prepared by diluting 10XPBS by ten times. pH was adjusted to 7.4.

TAE

Stock solution (50XTAE) was prepared by adding 121g Tris, 18.6g EDTA, and 28.55ml glacial acetic acid. The total volume was brought to 500ml with ddH_2O. Working solution (1XTAE) was prepared by diluting 50XTAE by 50 times.

DEPC-Treated Water

1ml DEPC was added to 1lt ddH_2O and stirred in a hood for 1 hour. The water was sterilized and DEPC was inactivated by autoclaving.

LB Medium

10g Tryptone, 10g NaCl and 5g Yeast Extract was dissolved in 1 lt ddH_2O. LB medium was sterilized by autoclaving.

LB-Agar

10g Tryptone, 10g NaCl, 5g Yeast Extract and 15g Bacto-Agar was dissolved in 1 lt ddH_2O. LB agar was sterilized by autoclaving. After the agar was cooled down to 55-60°C, desired antibody was added at a working concentration of 1X and 15-20ml LB-agar was poured into Petri plates aseptically.

Agarose Gel Loading Dye

0.009g BFB, 0.009g XC, 2.8mL ddH_2O and 1.2ml 0.5M EDTA was mixed. The total volume was brought to 15ml by adding glycerol.

1000X Ampicillin

Prepared as a stock solution of 100mg/ml concentration. Sterilized by filtration. 0.5ml aliqoutes were stored at -20°C.

1000X Kanamycin

Prepared as a stock solution of 25mg/ml concentration. Sterilized by filtration. 0.5ml aliqoutes were stored at -20°C.

5M NaOH

10g NaOH was dissolved in 50ml ddH_2O.

4% PFA

4g PFA was dissolved in 10ml 1XPBS by heating. The solution was kept at dark and freshly used when it comes 4°C.

5M NaCl

292.2g NaCl was dissolved in 1lt ddH_2O.

10%SDS

100g SDS was dissolved in 1lt ddH_2O by stirring.

1M Tris

60.55g Tris was dissolved in ∼300ml ddH_2O, 21ml 37% HCl was added. pH was adjusted to 8.0 with HCl, and the total volume was brought to 500ml by adding ddH_2O.

0.5M EDTA

93.05g EDTA was dissolved in ∼300ml ddH_2O by adjusting the pH to 8.0 with NaOH. After pH is adjusted, total volume was brought to 500ml by adding ddH_2O.

30% Acrylamide Mix

145g Acrylamide and 5g bis-acrylamide was dissolved in 500ml. The solution is filtered for 20 minutes. Acrylamide mix is stored in dark at 4°C.

SDS-PAGE Running Buffer

5X stock solution was prepared by dissolving 15g Tris, 73.2g Glycine and 5g SDS in 1lt ddH_2O. 1X working solution was prepared by diluting the stock solution 5 times. The stock and working solutions were kept at 4°C.

Wet Transfer Buffer

6g Tris, 28.8g Glycine, 1ml 10%SDS and 200ml Methanol was mixed and the total volume was brought to 1lt by adding ddH_2O.

Semi-Dry Transfer Buffer

5.8g Tris, 2.5g Glycine, 0.37g SDS and 200ml Methanol was mixed and the total volume was brought to 1lt by adding ddH_2O.

TBS

10X stock solution was prepared by dissolving 12.19g Tris and 87.76g NaCl in 1lt ddH_2O. 1X working solution was prepared by diluting 10XTBS 10 times. pH value of 1XTBS was brought to 7.50-7.65 with HCl addition.

TBS-T

1XTBS containing 0.3% Tween-20 was prepared and stored at 4°C.

Blocking Solution

2.5g dried milk was dissolved in 50ml TBS-T.

Bradford Reagent

100mg CBB was dissolved in 50ml 95%EtOH. 100ml phosphoric acid was added. Total volume was brought to 1lt with dH_2O. The reagent is filtered through Whatmann No:1 and stored in dark at 4°C.

Cracking Buffer (2X Protein Loading Buffer)

50 ml Cracking Buffer contaning; 50mM Tris(pH:6.8), 2mM EDTA (pH:8), 1% SDS, 20% Glycerol, 0,02%BFB was prepared. Prior to use 1% β-ME was added.

Camiolo Buffer (Protein Extraction Buffer)

0.368g KAc, 0.8765g NaCl, 1ml 0.5M EDTA, 125μl Triton-X100, and 0.871g L-arginine was mixed and brought to final volume of 50ml with ddH_2O. Buffer is sterilized by filtration.

Coomassie Staining Solution

Staining solution was prepared by dissolving 0.25g CBB in 45ml MeOH, 45ml ddH_2O, 10ml glacial acetic acid.

Coomassie Destaining Solution

Destaining solution containing 20%MeOH and 7% glacial acetic acid was prepared.

SSC

20X stock solution was prepared by dissolving 175.3g NaCl and 88.2 sodium citrate in 1lt ddH_2O. pH value was adjusted to 7.0 with NaOH.

Ponceau-S PVDF Membrane Staining Solution

0.05g Ponceau-S was dissolved in 50ml 5% acetic acid solution.

3.3 Cloning Studies

3.3.1 Cloning Strategy

The mouse and human *FLT3* genes have been previously cloned (Matthews *et al*, 1991; Rosnet *et al*, 1991; Rosnet *et al*, 1993). In order to clone the rat homologous of *FLT3* cDNA, the sequences of mouse and human genes were compared. The cDNA sequences of mouse *FLT3* (NM_010229), human *FLT3* (NM_004119), and predicted rat *FLT3* (XM_221874) were aligned using ClustalW tool (European Bioinformatics Institute).

We aimed to clone the full-length *FLT3* cDNA in three overlapping fragments. The primers were designed for the regions that are conserved among three species. The locations of the cloning primers is shown in Figure 3.1, and the sequences of the cloning primers are shown in Table 3.1.

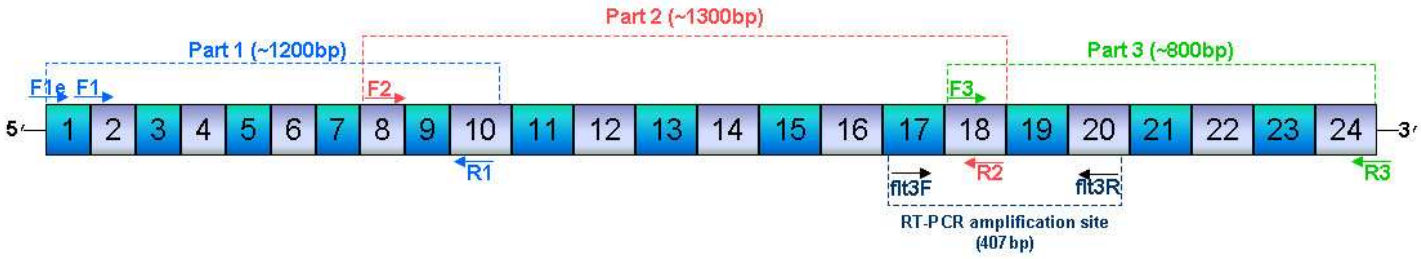

Figure 3.1: *Exons of FLT3 and Location of Cloning Primers. We aimed to clone rat homolog of FLT3 in three overlapping fragments. F1e and R1 primers (shown in blue) were used for amplifying Part1, F2 and R2 primers (shown in red) were used for amplifying Part2 and F3 and R3 primers (shown in green) were used for amplifying Part3. flt3F and flt3R primers, which were previously used to clone a partial cDNA of rat FLT3 gene (AY094358), were used for RT-PCR in this study.*

Primer	Sequence
F1e	5'-TCT AGA ATG CGG GCG TTG CG-3'
F1	5'-CTG CTT GTT GTT TTG TCA GTA ATG-3'
R1	5'-GGT TGT TCT TAT GAT CGC AAA ATT-3'
F2	5'-ACA GCG TTG GTG ACC ATC CTA-3'
R2	5'-GAA TTG AAT TCC CAT TGA ACC CTG-3'
F3	5'-GTT CAA TGG GAA TTC AAT TCA TTC-3'
R3	5'-TCT AGA CTA ACT TTT CTC TGT GAG-3'

Table 3.1: *Sequences of Cloning Primers*

3.3.2 Amplification and Purification of *FLT3* Fragments

Total cDNA from rat thymus was used as template for PCR amplifications. The PCR reaction conditions are shown in Table 3.2.

Reaction Mixture (25 μl reaction volume)	2 μl cDNA from rat thymus 10 pmol forward primer 10 pmol reverse primer 2,3 mM $MgCl_2$ (MBI Fermentas) 1,5 mM dNTP (MBI Fermentas) 2,5 μl 10X PCR Buffer (MBI Fermentas, Ontario, Canada) 1 unit Taq Polymerase (MBI Fermentas, Ontario, Canada)
PCR Reaction	95 °C 5 minutes 45 cycles { 94 °C 1 minute; 57 °C 1 minute; 72 °C 1 minute } 72°C 10 minutes

Table 3.2: *Reaction Conditions For Cloning of FLT3 Fragments*

After amplification, the amplified fragments were electrophoresed on agarose gel and purified from agarose gel with QIAquick Gel Extraction Kit (QIAGEN, Hilden, Germany). The DNA fragments were excised from the agarose gel. The excised parts were weighed. 3 volumes of Buffer QG was added to 1 volume of

gel, and incubated at 50°C for 10 minutes. 1 gel volume of isopropanol was added to the sample and mixed. The sample was applied to the QIAquick column, and centrifuged for 1 min at full speed. The column was washed by addition of 0.75 ml of Buffer PE, waiting for 5 minutes at room temperature and centrifuging for 1 min at full speed. The flow-through was discarded and the column was centrifuged for an additional 1 minute at full speed. The column was placed into a 1.5ml microcentrifuge tube. To elute the DNA 25-50μl of sterile ddH_2O was applied to the column, waited for 1 minute and centrifuged at full speed for 1 minute. The purified fragments were then sequenced (Iontek, Turkey).

3.3.3 Cloning of Amplified Fragments Into TA Cloning Vector

The fragments, Part 2 and Part 3, were cloned into pGEM-T Easy (Promega, Wisconsin, USA) cloning vector. The ligation reaction was prepared by mixing, 10μl 2X Rapid Ligation Buffer (Promega, Wisconsin, USA), 0,5μl pGEM-T Easy (25 ng), 8,5μl insert DNA and 1μl (3 Weiss units) T4 DNA Ligase (Promega, Wisconsin, USA). The mixture was incubated at 4°C for 48 hours.

After the ligation reactions the plasmids carrying the inserts were transformed into competent *E.coli* DH5α cells. The competent cells were kindly provided by Nuri Öztürk.

10μl of reaction mixture was added on 50μl of competent cells, and mixed by finger vortexing, gently. The mixture was incubated on ice for 30 minutes. Then, transformation mixture was incubated in 42°C for 90 seconds and on ice for 2 minutes. After ice incubation, 500μl LB medium was added and mixed by pipetting. The culture was incubated at 37°C for one hour. The cells were precipitated by centrifuging at 12000xg for 5 minutes. 400μl LB was discarded, and the cells were resuspended in the remaining medium. All the culture in the microfuge tube was plated to Ampicillin/X-Gal/IPTG plate. The plates were

incubated in a 37°C incubator overnight.

The white colonies on the plate were inoculated into 5ml LB containing 1X Ampicillin and incubated at 37°C for 8 hours. After 8 hours the plasmids were isolated by Plasmid Mini Kit (QIAGEN, Hilden, Germany). The orientation of the inserts were detected by restriction analysis. The *E.coli* clones that are carrying the sense and antisense insert DNA were inoculated into 5ml LB containing 1X Ampicillin, and incubated at 37°C for 8 hours. After 8 hours, glycerol stocks of the cultures were prepared by mixing 200μl sterile glycerol with 800μl culture. The glycerol stocks were stored at -80°C.

3.4 Liver Regeneration Models

3.4.1 Partial Hepatectomy and Sham Operations Alone

In this study, 9-week old male Sprague-Dawley rats were used. Our partial hepatectomy operations were performed based on the procedure standarized by Higgins and Anderson (1931).

3.4.1.1 70% Partial Hepatectomy Operation

The rats were anesthetized with Ketalar (Parke-Davis, Michigan, USA) and immobilized on the bench. After the sterilization with 70% ethanol, the skins were cut with a scissor. After removing the subcutaneous structures, the peritoneal membranes were cut carefully throughout the midline resulting in the opening of the abdomen. The PH operation is shown in Figure 3.2. Then the ligaments of the liver that connect the organ to the diaphragm, and the lobes to each other were cut. The middle lobe, which accounts for the 40% of the total liver mass,

and the front lobe, which accounts for the 30% of the total liver mass, was cut after the tying of the branch of vena cava inferior that enters to this lobe with silk. The color of this lobe immediately became dark after tying, which was due to the cutting of blood supply to this lobe. Then the lobe was washed in 1X PBS(DEPC-treated) and then quickly frozen in liquid nitrogen.

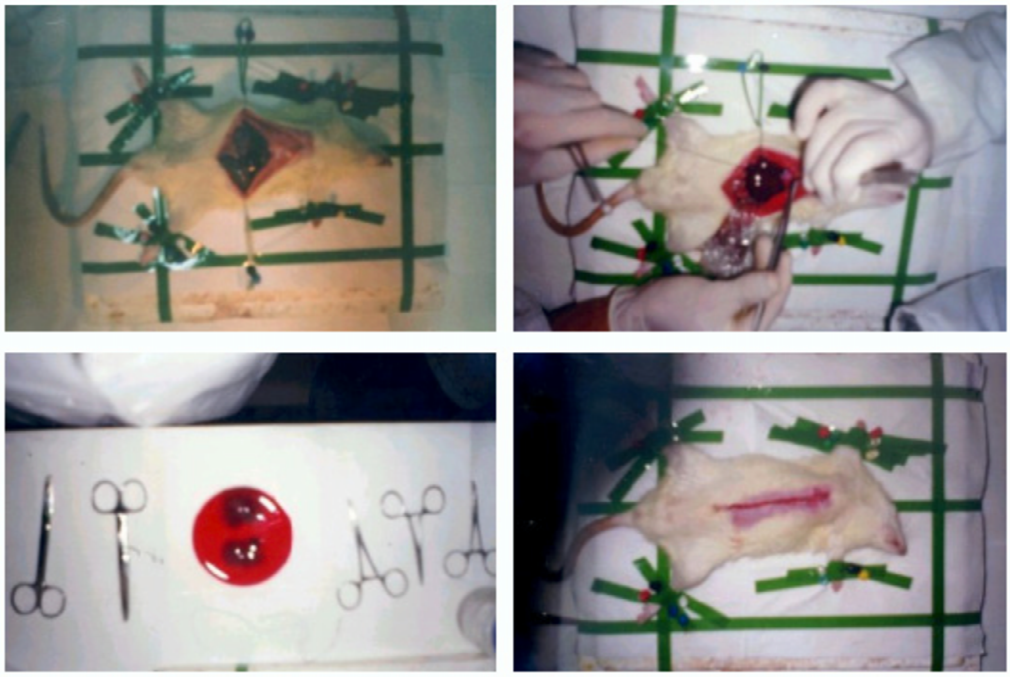

Figure 3.2: *The Liver Resection Surgery For PH*

After removing the lobe, the abdominal cavity of the animal was cleaned carefully. The intestines were placed to their original locations. Then the peritonea and the skin were closed separately by using propilen. After the completion of the surgery, the animals were placed under a lamp to increase its body temperature and then put into cages (one animal per cage) with continuous supply of food and water.

The animals were sacrificed; 30 minutes, 2 hours, 4 hours, 12 hours, 18 hours, 24 hours, 48 hours, 7 days and 14 days after operation. Their livers were taken, then frozen in liquid nitrogen and stored at -80°C.

3.4.1.2 Sham Operations

For the Sham group of animals, all the surgical operations were performed same as PH operations (Section 3.4.1.1), but the livers were not tied up and resected.

3.4.2 PH After AAF Treatment

AAF solution (125 mg/ml) was prepared in DMSO. Rats were weighed and 50 mg/kg AAF was administrated to each animal. Before injection desired amount of AAF solution was resuspended in corn oil to a final volume of 1 ml. AAF was administrated for 6 days by intraperitoneal injection. On 7^{th} day PH and SH operations were performed as described in Section 3.4.1.1 and 3.4.1.2, respectively. The animals were sacrificed 2 hours, 12 hours, 18 hours and 24 hours after operation. Two animals, one form PH group and one from SH group, were injected with AAF for 6 days after operation and these animals were sacrificed on 7^{th} day.

3.5 RNA Isolation and Quantification

3.5.1 RNA Isolation

During RNA isolations, all the solutions and materials were treated with DEPC in order to avoid RNase contamination. The total RNAs were isolated using Tripure solution (Roche/Boehringer Mannheim, Indiana, USA) according to the manufacturer's protocol. 100 mg of tissue samples were homogenized in 1 ml of Tripure solution by using the homogenizer. The homogenates were incubated for 5 minutes at room temperature for complete dissociation of the nucleoprotein complexes. Then 0.2 ml of chloroform added and shaken vigorously for 15 seconds. After incubating them at room temperature for 15 minutes, they were centrifuged at 12000xg for 40 minutes at 4°C. Three phase were occurred after centrifugation. The colorless upper aqueous phases were transferred to new eppendorf tubes and 1 ml of isopropanol was added on each sample. After mixing it by inverting the tubes several times, they were incubated at room temperature for 10 minutes. Then they were centrifuged at 12000xg for 15 minutes at 4°C and the supernatant were discarded. The pellets were washed with 1 ml of 75% ethanol, and then centrifuged at 7500xg for 5 minutes at 4°C. The supernatants were discarded and the pellets were air-dried on bench for about 10 minutes. The RNA pellets were resuspended in appropriate volume of the DEPC-treated water. The RNAs were stored at -80°C.

3.5.2 Quantification of RNA

The concentrations of RNA samples were measured via spectrophotometry. The integrity of the isolated RNA was controlled by agarose gel electrophoresis.

3.5.2.1 Spectrophotometry

1 μl of each samples were diluted 1:1000 with DEPC-treated ddH_2O. Then the OD measurements were done for 260 and 280 nm wavelengths with the spectrophotometer (Beckman, California, USA).

3.5.2.2 Agarose Gel Electrophoresis

Agarose gel electrophoresis was used to control the integrity of the isolated RNA. 1% agarose gel was prepared with 1X TAE Buffer, and 30 ng/ml ethidium bromide solution was added for visualization. Samples were prepared by addition of 1μl Agarose Gel Loading Dye, 3μl RNA sample and 6μl DEPC-treated H_2O. Samples were kept at 65°C for 10 minutes in order to denature the RNA molecules. Agarose gel was run at 100V for 30 minutes and visualized under transilluminator (Bio-Rad, California, USA). MultiAnalyst (Bio-Rad, California, USA) software was used to take photographs of the gels.

3.6 cDNA Synthesis

The cDNA samples were synthesized from the total RNA samples with the RevertAid First Strand cDNA Synthesis Kit (MBI Fermentas, Ontario, Canada) according to the manufacturer's protocol. 5 μg of RNA was mixed with 1 μl of oligo(dT) primer and ddH_2O in a total volume of 12 μl. They were incubated at 70°C for 5 minutes and then chilled on ice. Then 4 μl of 5x reaction buffer, 1 μl of Ribonuclease inhibitor and 2 μl of 10 mM dNTP mix were added and incubated at 37°C for 5 minutes. Finally, 1 μl of RevertAid M-MuLV reverse transcriptase were added and incubated at 42°C for 60 minutes. The reactions were stopped by heating at 70°C for 10 minutes, put into the ice and 20μl of ddH_2O was added to each sample. The cDNAs were stored at -20°C.

3.7 RT-PCR

3.7.1 Semi-Quantitative RT-PCR

Semi-quantitative RT-PCR is a suitable method for comparing relative amount of the used templates between different samples. In order to compare gene expression levels of samples with each other at RNA level, cyclophilin, a housekeeping gene, was used as a control of equal loading. Cyclophilin levels should be equal in cDNAs synthesized from equal amounts of RNA. The cycle number of RT-PCR reactions were optimized in order to detect the expression levels before saturation of the amplification. Quantification of amplicon intensities was performed using MultiAnalyst software. The primer sequences and reaction conditions for *CYC* and *FLT3* are shown in Table 3.3 and 3.4, respectively. The locations of the primers **flt3F** and **flt3R** are shown in Figure 3.3.

***CYC* Forward Primer**	5'-GGG AAG GTG AAA GAA GGC AT-3'
***CYC* Reverse Primer**	5'-GAG AGC AGA GAT TAC AGG GT-3'
Reaction Mixture	2 μl cDNA
(25 μl reaction volume)	10 pmol forward primer
	10 pmol reverse primer
	1,5 mM $MgCl_2$ (MBI Fermentas, Ontario, Canada)
	1,5 mM dNTP (MBI Fermentas, Ontario, Canada)
	2,5 μl 10X PCR Buffer (MBI Fermentas, Ontario, Canada)
	1 unit Taq Polymerase (MBI Fermentas, Ontario, Canada)
PCR Reaction	95 °C 5 minutes 18 cycles { 94 °C 30 seconds 55 °C 30 seconds 72 °C 30 seconds 72°C 10 minutes
Product size	211bp

Table 3.3: *Primer Sequences and Reaction Conditions for CYC*

flt3F	5'-TGG TGA CCT GCT CAA CTA CCTA-3'
flt3R	5'-AGT CAC AGA TCT TCA CCA CCTT-3'
Reaction Mixture	2 μl cDNA
(25 μl reaction volume)	5 pmol forward primer
	5 pmol reverse primer
	1,5 mM $MgCl_2$ (MBI Fermentas, Ontario, Canada)
	1,5 mM dNTP (MBI Fermentas, Ontario, Canada)
	2,5 μl 10X PCR Buffer (MBI Fermentas, Ontario, Canada)
	1 unit Taq Polymerase (MBI Fermentas, Ontario, Canada)
PCR Reaction	95 °C 5 minutes 35 cycles { 94 °C 30 seconds 60 °C 1 minute 72 °C 1 minute 72°C 10 minutes
Product size	407bp

Table 3.4: *Primer Sequences and Reaction Conditions for FLT3*

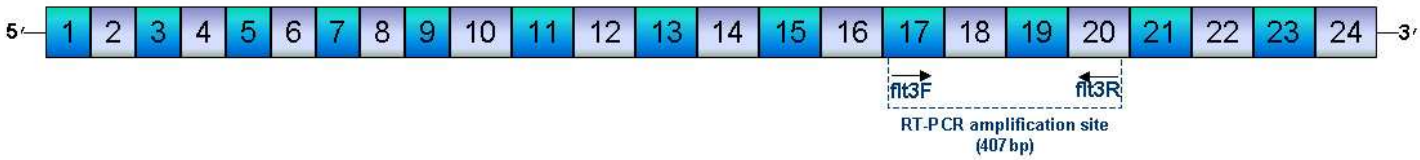

Figure 3.3: *Location of FLT3 Primers. flt3F and flt3R primers, which were previously used to clone a partial cDNA of rat FLT3 gene (AY094358), were used for RT-PCR in this study.*

3.7.2 Real-Time RT-PCR

The primers that are used for semi-quantitative RT-PCR (Section 3.7.1) also were used for real-time RT-PCR. Before the real-time RT-PCR reactions, the efficiencies of the primers were tested using a standard dilution series. The reaction conditions of real-time PCR are shown in Table 3.5.

The real-time PCR reactions were carried out in iCycler (Bio-Rad, California, USA). After the amplification steps a melting curve analysis was done.

AAF-treated samples were detected in duplicates, and the readings from each sample and its internal control (CYC) were used to calculate the gene expression level. The C_t value of gene expression collected through the amplification curves was used to analyze the relative expression level by using comperative C_t ($2^{-\Delta\Delta C_t}$) method (Livak and Schmittgen, 2001). Normal liver was used as a calibrator for this method. The results of real-time RT-PCR were compared with the results of semi-quantitative RT-PCR by using CORRELLATION function of Excel software (Microsoft).

Reaction Mixture for FLT3 **(12.5 μl total reaction volume)**	1 μl cDNA 5 pmol forward primer 5 pmol reverse primer 6.25 μl iQ SyBr Green Super Mix (Bio-Rad)
Real-Time PCR Reaction of FLT3	95 °C 10 minutes 50 cycles { 94 °C 1 minute 60 °C 1 minute 72 °C 1 minute 72°C 10 minutes
Reaction Mixture for CYC **(12.5 μl total reaction volume)**	1 μl cDNA 10 pmol forward primer 10 pmol reverse primer 6.25 μl iQ SyBr Green Super Mix (Bio-Rad)
Real-Time PCR Reaction of CYC	95 °C 10 minutes 32 cycles { 94 °C 30 seconds 55 °C 30 seconds 72 °C 30 seconds 72°C 10 minutes

Table 3.5: *Reaction Conditions For Real-Time RT-PCR*

3.8 Protein Isolation and Quantification

100 mg of tissue samples were homogenized in 1 ml of Camiolo Buffer by using the homogenizer. The homogenates were centrifuged at 12000xg for 20 minutes at 4°C. The supernatant which contains the proteins were taken into a new tube.

The concentration of protein samples were measured with Bradford assay. According to the results of Bradford assay, proteins were diluted to a concentration of 6μg/μl. The protein samples were stored at -80°C.

In order to check the equal loading, 12 μg of protein samples were run on 8% SDS polyacrylamide gel. For preparing the protein samples, 2μl protein, 3μl ddH_2O and 5μl Cracking Buffer containing 1% β-ME was mixed and boiled for 5 minutes. 5μl PageRuler Prestained Protein Ladder (MBI Fermentas, Ontario, Canada) was used as protein molecular weight marker. After electrophoresis, the gel was stained with Coomassie Staining Solution for 5 minutes and then destained with Coomassie Destaining Solution overnight. After destaining, the gel was dried at 60°C for 45 minutes, and fixed on Whatmann paper.

3.9 Western Blotting

The proteins were separated on 8% SDS polyacrylamide as described in Section 3.8. After the electrophoresis, the proteins were transferred to PVDF membrane (Roche, Indiana, USA). The transfer was performed in wet-transfer buffer, at 14V, at 4°C overnight. After the transfer is completed the success of the transfer was controlled by staining the membrane with Ponceau-S PVDF membrane staining solution for 5 minutes, and destaining with water until the protein bands became visible. After this step the membrane was destained completely with water, and blotting steps were performed.

The membrane was blocked with blocking solution for 1 hour at room temperature on an orbital shaker. FLT3 antibody (Santa Cruz, California, USA) was diluted to a concentration of 0.2 μg/ml in blocking solution, and the membrane was incubated in antibody solution for 1 hour at room temperature on an orbital shaker. Then, the membrane was washed with TBS-T. After washing steps the secondary antibody, Anti-Rabbit-HRP (Sigma, Montana, USA), was diluted 5000 times in blocking solution, and the membrane was incubated in secondary antibody solution for 1 hour at room temperature on an orbital shaker. After secondary antibody step, the membrane was washed with TBS-T.

After the washing step membrane was incubated with ECL Plus Detection Reagent (Amersham Biosciences, New Jersey, USA) for 5 minutes. The excess detection reagent was drained off, and the membrane was placed on glass and covered with SaranWrap. The wrapped glass was placed in a x-ray film cassette. X-ray films were exposed for 5 seconds, 10 seconds, 30 seconds, 1 minute and 3 minutes. After exposure the films were developed.

3.10 Immunohistochemistry

After the liver tissues were taken from the animals, they were soaked in 1XPBS and then fixed in 10% neutral phosphate-buffered formalin. After formalin fixation, the tissues were dehydrated and embedded into paraffin and stored at room temperature. For immunohistochemistry 7μm sections were taken. The sections were deparafinized by incubating at 60°C for 20 minutes and keeping in xylene for 5 minutes. After deparaffinization, tissue sections were rehydrated by immersing them into 100%, 95%, 80%, 65%, 50%, 40%, and 30% ethanol for 2 minutes each, respectively, and then the sections were immersed in dH_2O for 2 minutes. After deparaffinization and rehydration steps, in order to quench endogenous peroxidase activity, the tissue sections were incubated in 3% H_2O_2 for 25 minutes.

After H_2O_2 step, the sections were washed with 1XPBS and the specimen were blocked with 2% BSA for 1 hour at room temperature in humid chamber.

Primary antibody, FLT3 antibody (Santa Cruz, California, USA), was diluted to 5μg/ml in 1% BSA, and the specimen were covered with primary antibody solution and incubated for overnight at 4°C in humid chamber. After primary antibody incubation, the sections were washed with 1XPBS and incubated with Biotinylated Link Anti-Mouse & Anti-Rabbit Ig (DakoCytomation, Glostrup, Denmark) for 15 minutes at room temperature. Then the sections were washed with 1XPBS and incubated with Streptavidin-HRP (DakoCytomation, Glostrup, Denmark) for 15 minutes at room temperature, and the sections were washed with 1XPBS.

After washing step, the specimen were covered with Liquid DAB+ Substrate (DakoCytomation, Glostrup, Denmark) and incubated for 10-15 seconds and immediately washed with dH_2O. After substrate step the specimen were counterstained with hematoxylin for 30 seconds, rinsed with dH_2O, and washed with tap water. After the washing step the specimen were mounted using Faramount Aqueous Mounting Medium (DakoCytomation, Glostrup, Denmark), and coverslipped.

Chapter 4

Results

4.1 Cloning Studies

We aimed to clone the rat homolog of *FLT3* cDNA in three overlapping fragments (Part1, Part2, Part3) (Figure 4.1).

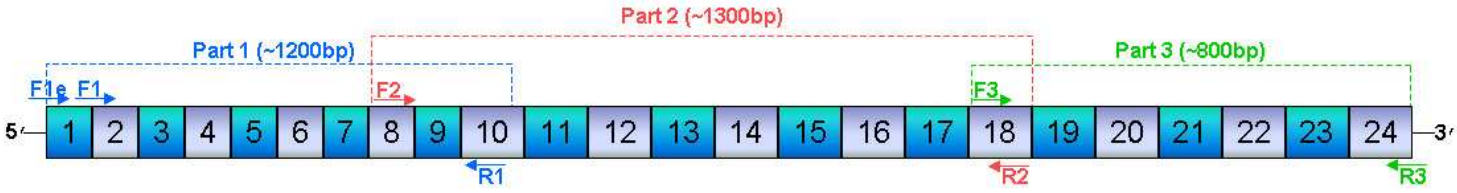

Figure 4.1: *Location of Cloning Primers. F1e and R1 primers (shown in blue) were used for amplifying Part1, F2 and R2 primers (shown in red) were used for amplifying Part2 and F3 and R3 primers (shown in green) were used for amplifying Part3.*

Part1, Part2 and Part3 of rat *FLT3* cDNA were amplified from thymus. The first attempt of amplifying Part1 with primers F1e and R1 was not successful since the beginning of the coding region was GC rich and we could not manage optimization of PCR conditions for this primer set. Then a second forward primer F1 that recognizes a sequence which is located approximately 35 bases

after the beginning of the coding region was designed, and Part1 was amplified with primers F1 and R1 (Figure 4.2).

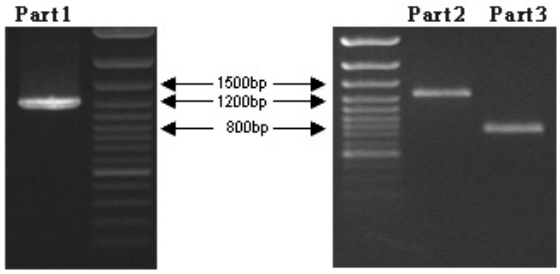

Figure 4.2: *Agarose Gel Electrophoresis of PCR Products Part1, Part2 and Part3. All the fragments were amplified from thymus cDNA. The sizes of the amplified fragments were expected. 100bp DNA Ladder Plus (MBI Fermentas) was used as molecular size marker.*

The amplified fragments were sequenced. Combining the sequence analysis results of Part1, Part2, and Part3, along with a small fragment we previously cloned (AY94358), we were able to determine a partial cDNA sequence for rat homolog of *FLT3* gene (Figure 4.3).

Obtained partial sequence of rat *FLT3* was aligned with mouse *FLT3* (NM_010229) and human *FLT3* (NM_004119) (Figure 4.4), and aligned with a predicted rat *FLT3* sequence (XM_221874) (Figure 4.5) by BCM Search Launcher: Multiple Sequence Alignments tool (Baylor College of Medicine). The partial sequence showed 90% homology with mouse sequence and 81% homology with human sequence. When the alignment data is considered, we saw that ∼80 bases from the beginning of the coding region were missing from our partial sequence in comparison to mouse and human sequences. In the alignment between rat and predicted rat sequences; we saw that there were gaps in alignment. The predicted sequence constructed by gene scan was including some regions that did not correspond to our sequencing results.

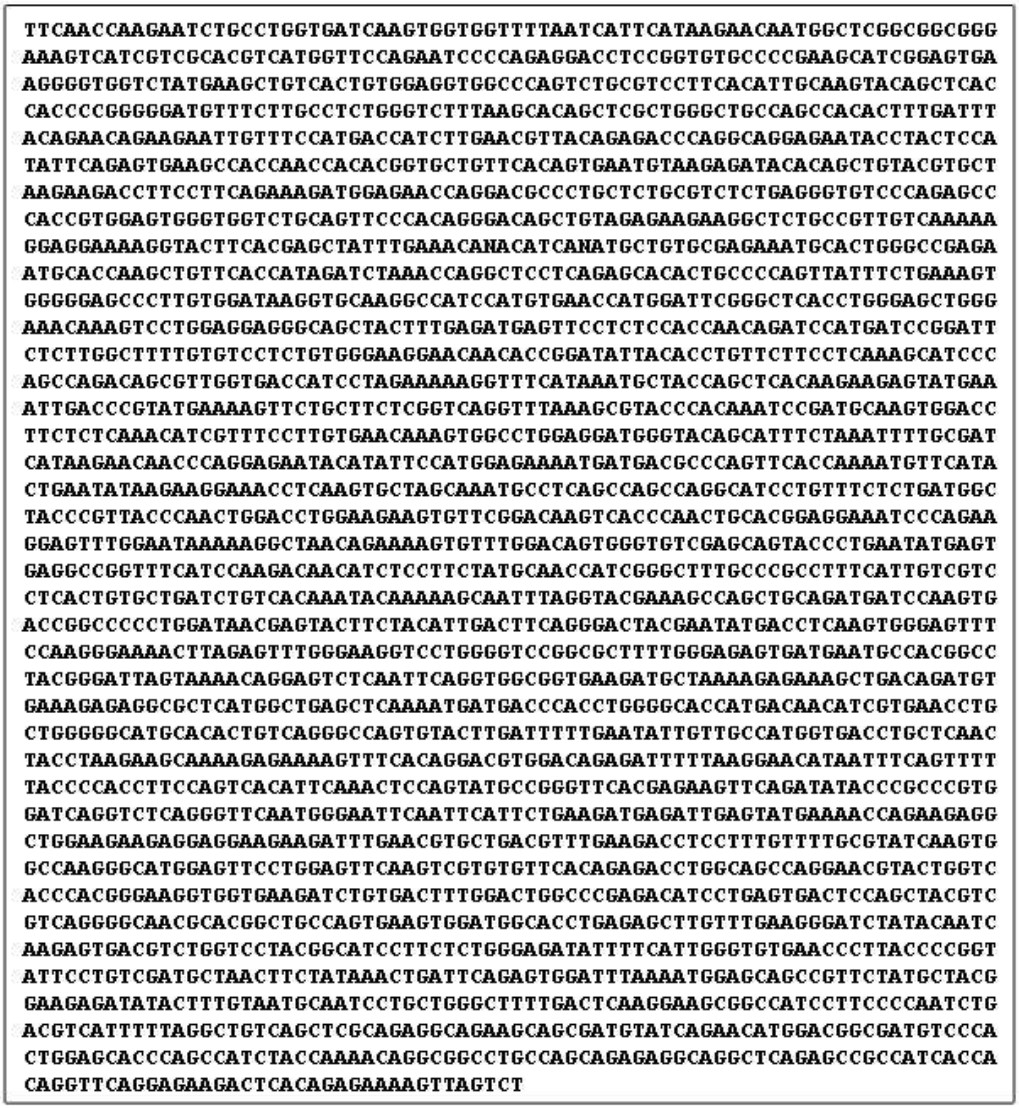

Figure 4.3: *Partial Sequence of Rat Homolog of FLT3 cDNA*

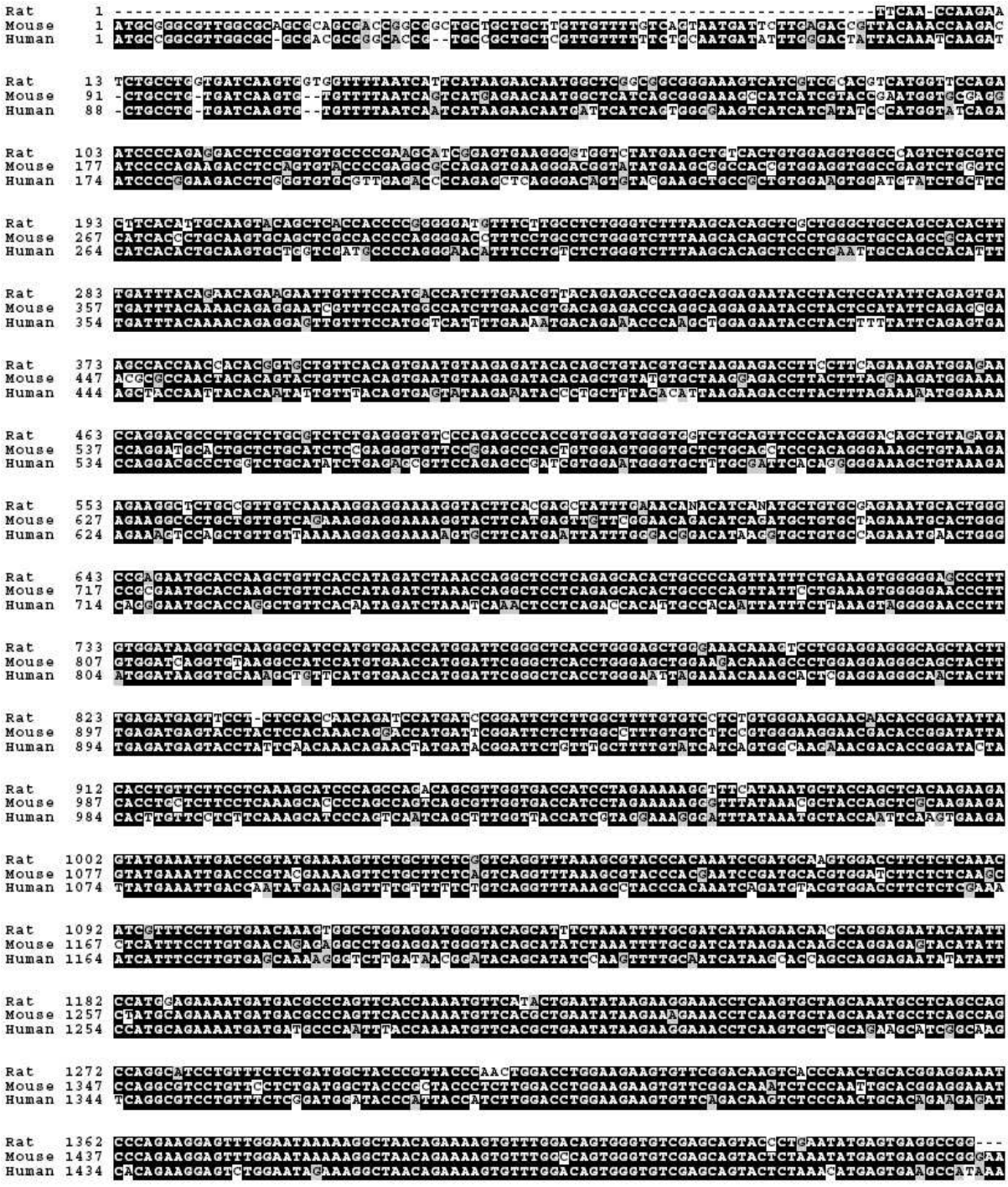

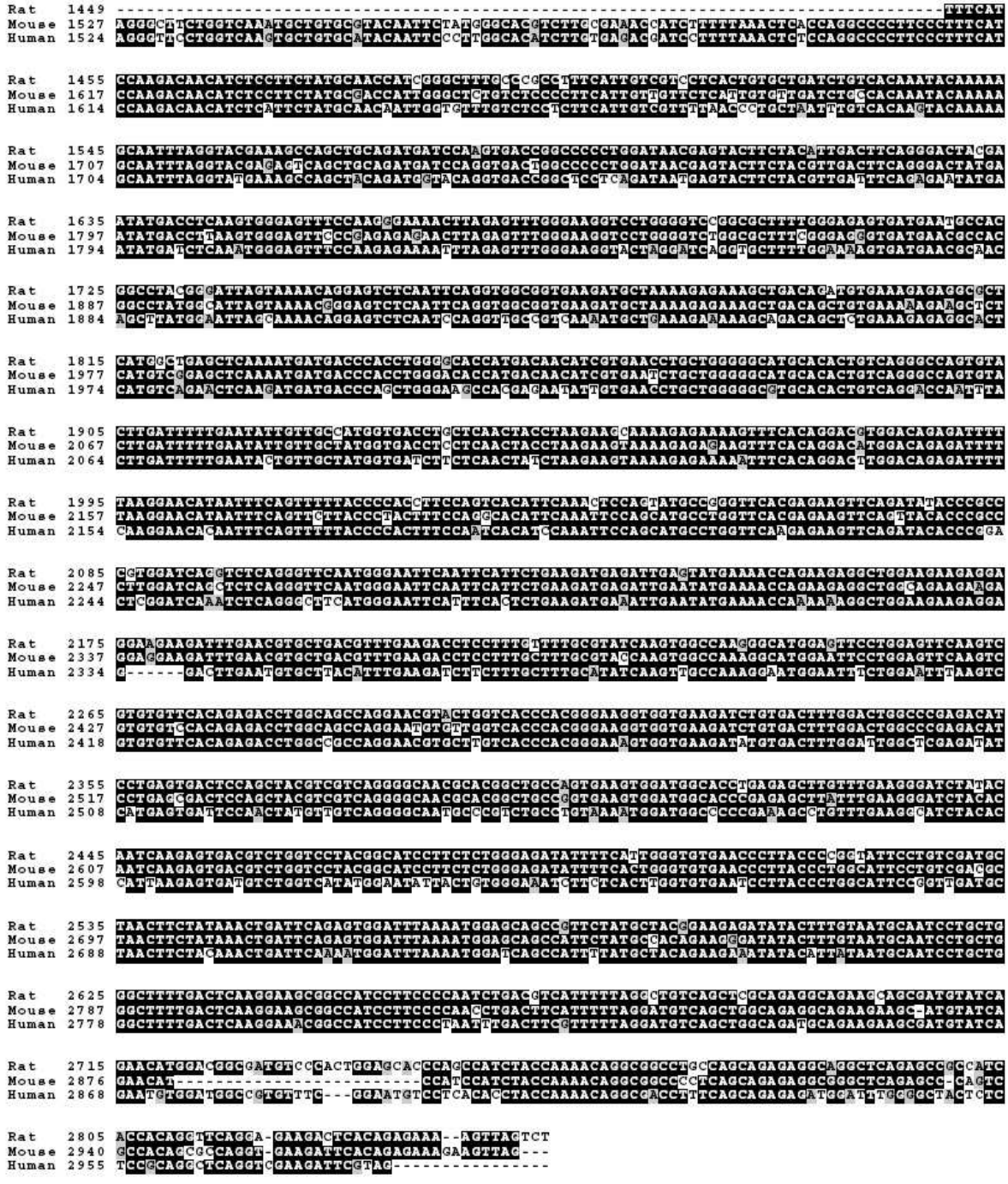

Figure 4.4: *Comparison of Rat, Mouse (NM_010229) and Human (NM_004119) FLT3 cDNAs. The regions that are conserved in all three species are shown in black blocks.*

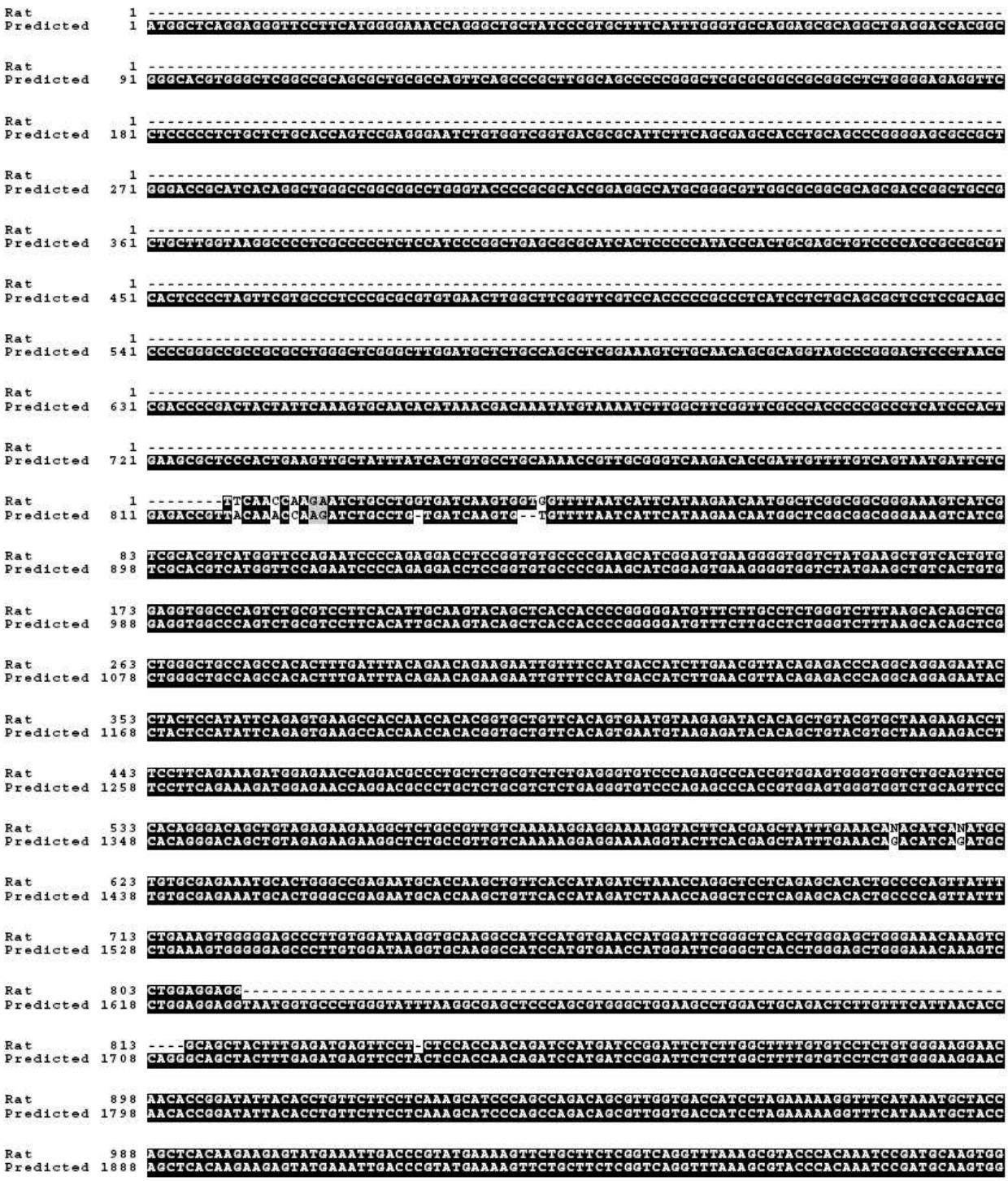
Rat 1 ----------
Predicted 1 ATGGCTCAGGAGGGTTCCTTCATGGGGAAACCAGGGCTGCTATCCCGTGCTTTCATTTGGGTGCCAGGAGCGCAGGCTGAGGACCACGGC
Rat 1 ----------
Predicted 91 GGGCACGTGGGCTCGGCCGCAGCGCTGCGCCAGTTCAGCCCGCTTGGCAGCCCCCGGGCTCGCGCGGCCGCGGCCTCTGGGGAGAGGTTC
Rat 1 ----------
Predicted 181 CTCCCCCTCTGCTCTGCACCAGTCCGAGGGAATCTGTGGTCGGTGACGCGCATTCTTCAGCGAGCCACCTGCAGCCCGGGGAGCGCCGCT
Rat 1 ----------
Predicted 271 GGGACCGCATCACAGGCTGGGCCGGCGGCCTGGGTACCCCGCGCACCGGAGGCCATGCGGGCGTTGGCGCGGCGCAGCGACCGGCTGCCG
Rat 1 ----------
Predicted 361 CTGCTTGGTAAGGCCCCTCGCCCCCTCTCCATCCCGGCTGAGCGCGCATCACTCCCCCATACCCACTGCGAGCTGTCCCCACCGCCGCGT
Rat 1 ----------
Predicted 451 CACTCCCCTAGTTCGTGCCCTCCCGCGCGTGTGAACTTGGCTTCGGTTCGTCCACCCCCGCCCTCATCCTCTGCAGCGCTCCTCCGCAGC
Rat 1 ----------
Predicted 541 CCCCGGGCCGCCGCGCCTGGGCTCGGGCTTGGATGCTCTGCCAGCCTCGGAAAGTCTGCAACAGCGCAGGTAGCCCGGGACTCCCTAACC
Rat 1 ----------
Predicted 631 CGACCCCGACTACTATTCAAAGTGCAACACATAAACGACAAATATGTAAAATCTTGGCTTCGGTTCGCCCACCCCCGCCCTCATCCCACT
Rat 1 ----------
Predicted 721 GAAGCGCTCCCACTGAAGTTGCTATTTATCACTGTGCCTGCAAAACCGTTGCGGGTCAAGACACCGATTGTTTTGTCAGTAATGATTCTC
Rat 1 --------TTCAACCAAGAATCTGCCTGGTGATCAAGTGGTGGTTTTAATCATTCATAAGAACAATGGCTCGGCGGCGGCGAAAGTCATCG
Predicted 811 GAGACCGTTACAAACCAAGATCTGCCTG-TGATCAAGTG--TGTTTTAATCATTCATAAGAACAATGGCTCGGCGGCGGCGAAAGTCATCG
Rat 83 TCGCACGTCATGGTTCCAGAATCCCCAGAGGACCTCCGGTGTGCCCCGAAGCATCGGAGTGAAGGGGTGGTCTATGAAGCTGTCACTGTG
Predicted 898 TCGCACGTCATGGTTCCAGAATCCCCAGAGGACCTCCGGTGTGCCCCGAAGCATCGGAGTGAAGGGGTGGTCTATGAAGCTGTCACTGTG
Rat 173 GAGGTGGCCCAGTCTGCGTCCTTCACATTGCAAGTACAGCTCACCACCCCGGGGGATGTTTCTTGCCTCTGGGTCTTTAAGCACAGCTCG
Predicted 988 GAGGTGGCCCAGTCTGCGTCCTTCACATTGCAAGTACAGCTCACCACCCCGGGGGATGTTTCTTGCCTCTGGGTCTTTAAGCACAGCTCG
Rat 263 CTGGGCTGCCAGCCACACTTTGATTTACAGAACAGAAGAATTGTTTCCATGACCATCTTGAACGTTACAGAGACCCAGGCAGGAGAATAC
Predicted 1078 CTGGGCTGCCAGCCACACTTTGATTTACAGAACAGAAGAATTGTTTCCATGACCATCTTGAACGTTACAGAGACCCAGGCAGGAGAATAC
Rat 353 CTACTCCATATTCAGAGTGAAGCCACCAACCACACGGTGCTGTTGACAGTGAATGTAAGAGATACACAGCTGTACGTGCTAAGAAGACCT
Predicted 1168 CTACTCCATATTCAGAGTGAAGCCACCAACCACACGGTGCTGTTCACAGTGAATGTAAGAGATACACAGCTGTACGTGCTAAGAAGACCT
Rat 443 TCCTTCAGAAAGATGGAGAACCAGGACGCCCTGCTCTGCGTCTCTGAGGGTGTCCCAGAGCCCACCGTGGAGTGGGTGGTCTGCAGTTCC
Predicted 1258 TCCTTCAGAAAGATGGAGAACCAGGACGCCCTGCTCTGCGTCTCTGAGGGTGTCCCAGAGCCCACCGTGGAGTGGGTGGTCTGCAGTTCC
Rat 533 CACAGGGACAGCTGTAGAGAAGAAGGCTCTGCCGTTGTCAAAAAGGAGGAAAAGGTACTTCACGAGCTATTTGAAACANACATCANATGC
Predicted 1348 CACAGGGACAGCTGTAGAGAAGAAGGCTCTGCCGTTGTCAAAAAGGAGGAAAAGGTACTTCACGAGCTATTTGAAACAGACATCAGATGC
Rat 623 TGTGCGAGAAATGCACTGGGCCGAGAATGCACCAAGCTGTTCACCATAGATCTAAACCAGGCTCCTCAGAGCACACTGCCCCAGTTATTT
Predicted 1438 TGTGCGAGAAATGCACTGGGCCGAGAATGCACCAAGCTGTTCACCATAGATCTAAACCAGGCTCCTCAGAGCACACTGCCCCAGTTATTT
Rat 713 CTGAAAGTGGGGGAGCCCTTGTGGATAAGGTGCAAGGCCATCCATGTGAACCATGGATTCGGGCTCACCTGGGAGCTGGGAAACAAAGTC
Predicted 1528 CTGAAAGTGGGGGAGCCCTTGTGGATAAGGTGCAAGGCCATCCATGTGAACCATGGATTCGGGCTCACCTGGGAGCTGGGAAACAAAGTC
Rat 803 CTGGAGGAGG----------
Predicted 1618 CTGGAGGAGGTAATGGTGCCCTGGGTATTTAAGGCGAGCTCCCAGCGTGGGCTGGAAGCCTGGACTGCAGACTCTTGTTTCATTAACACC
Rat 813 ----GCAGCTACTTTGAGATGAGTTCCT-CTCCACCAACAGATCCATGATCCGGATTCTCTTGGCTTTTGTGTCCTCTGTGGGAAGGAAC
Predicted 1708 CAGGGCAGCTACTTTGAGATGAGTTCCTACTCCACCAACAGATCCATGATCCGGATTCTCTTGGCTTTTGTGTCCTCTGTGGGAAGGAAC
Rat 898 AACACCGGATATTACACCTGTTCTTCCTCAAAGCATCCCAGCCAGACAGCGTTGGTGACCATCCTAGAAAAAGGTTTCATAAATGCTACC
Predicted 1798 AACACCGGATATTACACCTGTTCTTCCTCAAAGCATCCCAGCCAGACAGCGTTGGTGACCATCCTAGAAAAAGGTTTCATAAATGCTACC
Rat 988 AGCTCACAAGAAGAGTATGAAATTGACCCGTATGAAAAGTTCTGCTTCTCGGTCAGGTTTAAAGCGTACCCACAAATCCGATGCAAGTGG
Predicted 1888 AGCTCACAAGAAGAGTATGAAATTGACCCGTATGAAAAGTTCTGCTTCTCGGTCAGGTTTAAAGCGTACCCACAAATCCGATGCAAGTGG

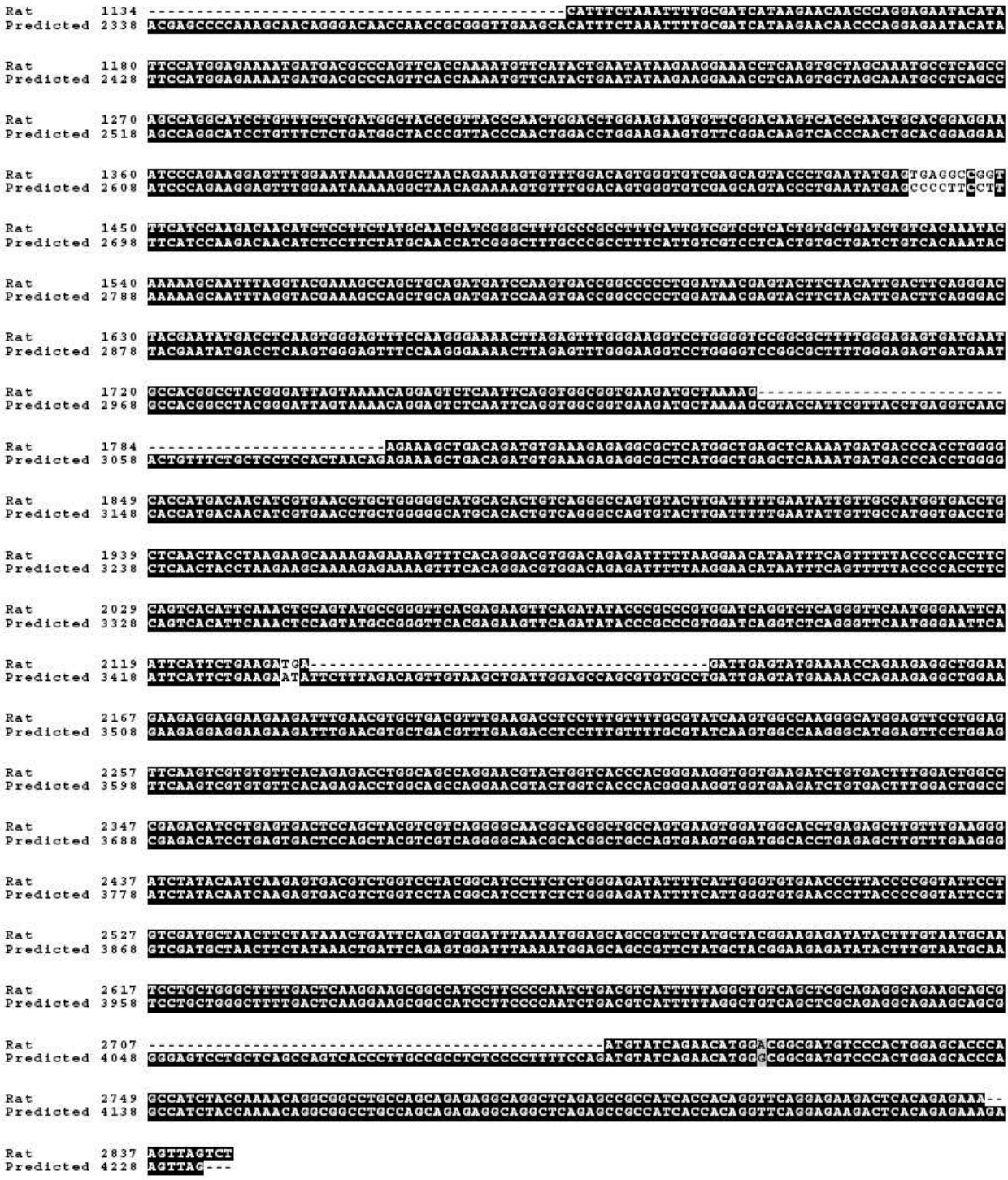

Figure 4.5: *Comparison of Rat and Predicted Rat (XM_221874) FLT3 cDNAs. The regions that are conserved in all three species are shown in black blocks.*

4.2 Tissue Specific Expression of FLT3

We analyzed the expression of FLT3 in different rat tissues both at mRNA (Figure 4.6) and protein (Figure 4.7) level. For this purpose, female and male rats were sacrificed and their tissues were collected. RNA isolation and RT-PCR were performed as explained in Section 3.5, 3.6, and 3.7. Protein isolation and Western blotting were performed as explained in Section 3.8 and 3.9.

Our results showed that, although FLT3 expression at mRNA level was seen in all the tissues, the expression level was not the same (Figure 4.6). In uterus, spleen, cerebellum and lungs the expression of FLT3 was higher, whereas in brain, ovary and skeletal muscle FLT3 level remained rather low.

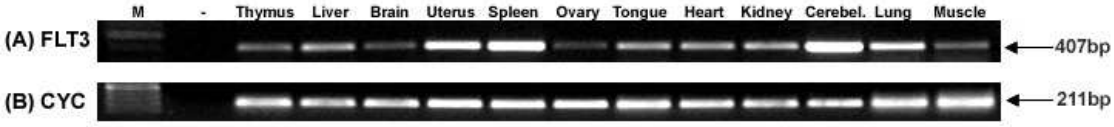

Figure 4.6: *The Expression of (A)FLT3 and (B)CYC In Different Rat Tissues. M: 100bp DNA Ladder Plus (MBI Fermentas, Ontario, Canada), -: the negative control*

In contrast to presence of FLT3 mRNA in heart and kidney (Figure 4.6), we did not detect any expression at protein level in these tissues (Figure 4.7A, first two lanes). Furthermore, in all the tissues, except liver, the FLT3 band corresponded to ∼150-160 kDa, whereas in liver the FLT3 band corresponded to ∼130-140 kDa.

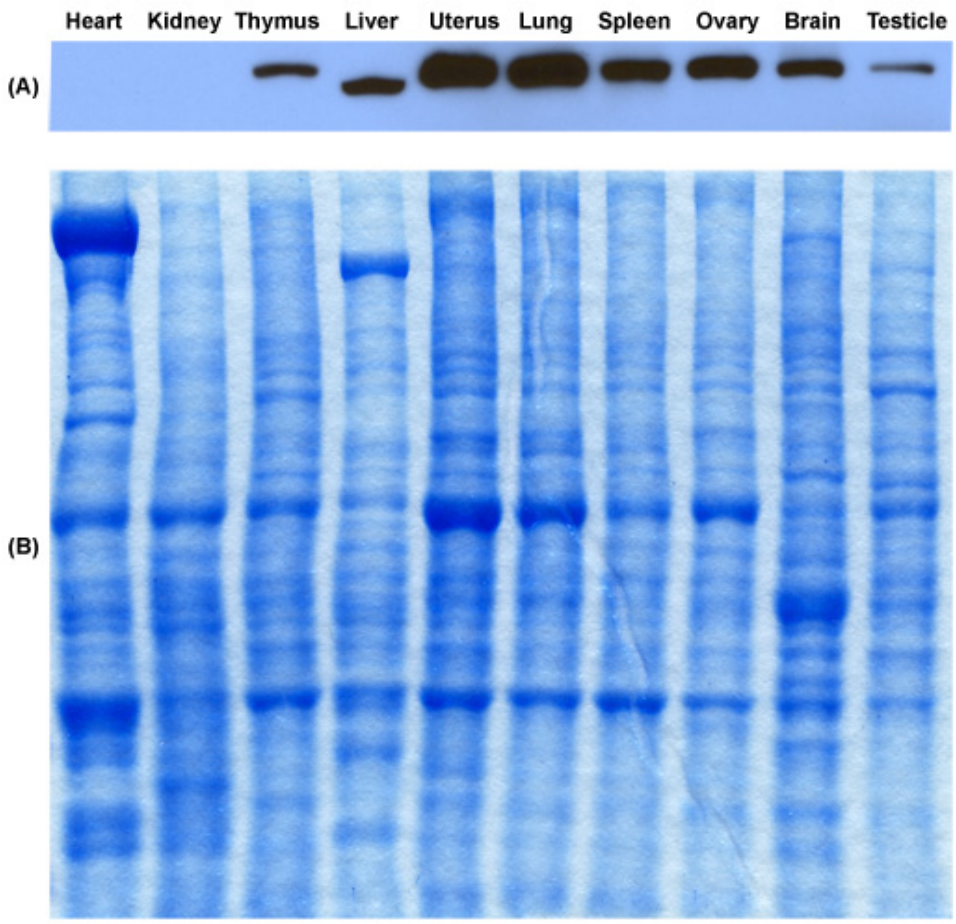

Figure 4.7: *Western Blot of Proteins From Different Rat Tissues. (A) Western blotting of different rat tissue proteins with anti-FLT3 antibody and (B) the Coomassie staining of SDS-PAGE of same proteins.*

4.3 Semi-Quantitative RT-PCR Results

4.3.1 Expression of FLT3 in SH and PH Groups

The expression of FLT3 at mRNA level in SH and PH groups were analyzed by semi-quantitative RT-PCR. PH and SH operations were performed as explained in Section 3.4.1. 30 minutes, 2 hours, 4 hours, 12 hours, 18 hours, 24 hours, 48 hours, 7 days and 14 days after operations, a single rat from PH group and another from SH group were sacrificed and their liver tissues were collected. RNA isolation, cDNA synthesis and RT-PCR were performed as explained in Section 3.5, 3.6, and 3.7. The PCR products were run on agarose gel (Figure 4.8).

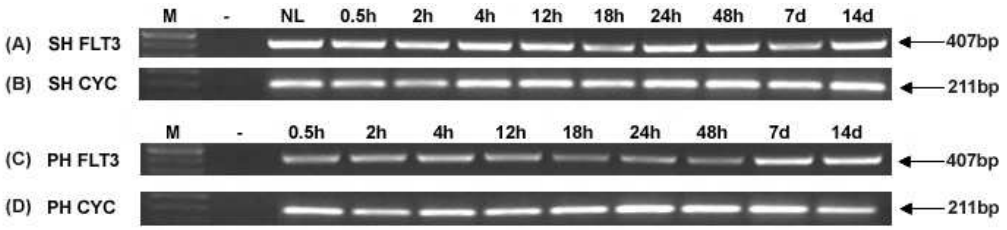

Figure 4.8: *Expression of FLT3 in SH and PH Groups. M: 100bp DNA Ladder Plus, - : is the negative control, and NL: normal liver sample. (A) FLT3 amplification in SH groups, (B) CYC amplification in SH groups, (C) FLT3 amplification in PH groups, and (D) CYC amplification in PH Groups*

The quantification results for SH and PH groups are given in Table 4.1. Relative expression of FLT3 was calculated in comparison to the expression of CYC.

In SH groups a slight but consistent decrease in FLT3 expression over the period of regeneration was apperant. In PH groups a similar pattern was observed but to a greater degree than that observed in SH groups. The expression was then increased after 18 hours (Figure 4.9).

NAME	*FLT3 Density*	*CYC Density*	*Relative Expression*
NL	12830,26	13479,02	100,00
SH 2h	10925,66	11362,50	101,02
SH 12h	11543,75	15498,81	78,25
SH 18h	8485,86	14201,79	62,77
SH 24h	11670,72	16323,21	75,11
SH 7d	8651,64	15186,31	59,85
NL	12830,26	13479,02	100,00
PH 2h	8265,38	12358,93	70,26
PH 12h	7429,06	13842,26	56,38
PH 18h	4753,85	14788,10	33,77
PH 24h	6242,74	17483,33	37,51
PH 7d	12017,99	16773,21	75,27

Table 4.1: *Quantification of Semi-Quantitative PCR Results for SH and PH Groups.*

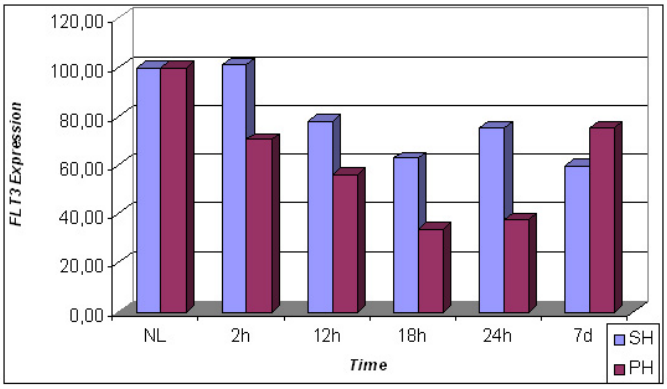

Figure 4.9: *FLT3 expression in SH and PH Groups*

4.3.2 Expression of FLT3 in AAF-Treated SH and PH Groups

The expression of FLT3 at mRNA level in AAF-treated SH and PH groups were analyzed by semi-quantitative RT-PCR. AAF treatment, followed by PH and SH operations were performed as explained in Section 3.4.2. 2 hours, 12 hours, 18 hours, 24 hours, and 7 days after operations, one rat from PH group and one rat from SH group were sacrificed and their liver tissues were collected. RNA isolation and RT-PCR were performed as explained in Section 3.5, 3.6, and 3.7. The PCR products were run on agarose gel (Figure 4.10).

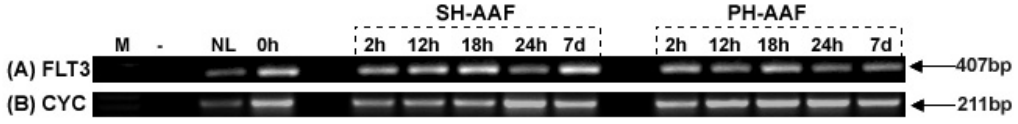

Figure 4.10: *Expression of FLT3 in AAF-Treated SH and PH Groups. M: 100bp DNA Ladder Plus, - : the negative control, NL: normal liver sample, and 0h: liver sample taken from an AAF-treated animal which is not subjected to PH. (A) FLT3 amplification in AAF-treated SH and PH groups,and (B) CYC amplification in AAF-treated SH and PH groups.*

The quantification results for AAF-treated SH and PH groups are given in Table 4.2. Relative expression of FLT3 was calculated in comparison to expression of CYC.

In AAF-treated SH groups, except 24 hours groups there was a slight decrease in FLT3 mRNA level (Figure 4.11). In AAF-treated PH groups, FLT3 mRNA level appeared to have decreased starting from 2 hours.

NAME	***FLT3 Density***	***CYC Density***	***Relative Expression***
NL	4735,19	7227,02	100,00
AAF 0h	10321,30	15286,29	103,05
SH-AAF 2h	8476,85	11795,97	109,68
SH-AAF 12h	9796,30	12124,19	123,32
SH-AAF 18h	11250,93	13402,82	128,12
SH-AAF 24h	6890,74	16808,47	62,57
SH-AAF 7d	11671,30	15207,66	117,13
PH-AAF 2h	9240,74	14517,74	97,15
PH-AAF 12h	7395,37	15881,85	71,07
PH-AAF 18h	9538,89	15984,68	91,08
PH-AAF 24h	6277,78	16212,90	59,10
PH-AAF 7d	7037,96	14235,89	75,45

Table 4.2: *Quantification of Semi-Quantitative PCR Results for AAF-Treated SH and PH Groups*

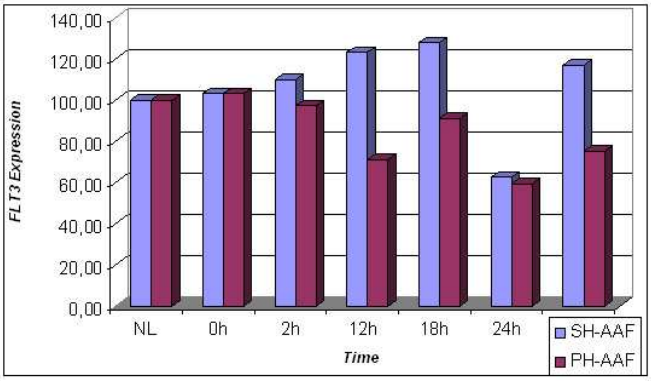

Figure 4.11: *FLT3 expression in AAF-Treated SH and PH Groups*

4.4 Real-Time RT-PCR Results

For real-time RT-PCR studies the cDNA samples which were used for semi-quantitative RT-PCR of SH, PH, AAF-treated SH, and AAF-treated PH groups were used. The real-time PCR reactions were performed as explained in Section 3.7.2. Efficiency of CYC and FLT3 primers were tested, standard curves were derived and E values were calculated for both primer sets. Since E values of CYC and FLT3 were 1,9 and 1,95, respectively, the E values were accepted as 2 for calculations.

4.4.1 Expression of FLT3 in SH and PH Groups

The C_t values of SH and PH groups (normal liver, 2 hours, 12 hours, 18 hours, 24 hours and 7 days) for both *FLT3* and *CYC* were collected. The C_t values of the PH groups were normalized according to the difference between the C_t values of normal liver samples in both groups. By using normalized C_t values, ΔC_t ($\Delta C_{t_{FLT3}} - \Delta C_{t_{CYC}}$) value for each group was calculated. Fold change in expression of *FLT3* was calculated by using $2^{-(\Delta C_t - \Delta C_{t_{NL}})}$ formula. For calculation, ΔC_t of normal liver sample was used as calibrator. Table 4.3 and Table 4.4 show the real-time RT-PCR data and the results of the calculations for SH and PH groups, respectively. Figure 4.12 and figure 4.13 show the fold changes of FLT3 expression graphics for SH and PH groups, respectively.

Real-time PCR quantifications showed that, FLT3 expression pattern of SH groups (Figure 4.12) is consistent with semi-quantitative PCR results (Figure 4.9). The correlation value of semi-quantitative RT-PCR and real-time RT PCR-was 0,99 for SH groups. Also, quantifications of PH groups (Figure 4.13) was similar with semi-quantitative PCR of PH groups (Figure 4.9). The correlation value was 0,88 for PH groups.

NAME	***FLT3 C_t***	***CYC C_t***	ΔC_t	$2^{-(\Delta C_t - \Delta C_{t_{NL}})}$
NL	22,7	13,3	9,4	1,00
SH 2h	23,2	13,5	9,7	0,81
SH 12h	23,2	13,1	10,1	0,62
SH 18h	24,3	13,8	10,5	0,47
SH 24h	23,3	13,1	10,2	0,57
SH 7d	24,3	13,7	10,6	0,44

Table 4.3: *Real-Time RT-PCR Data For SH Groups*

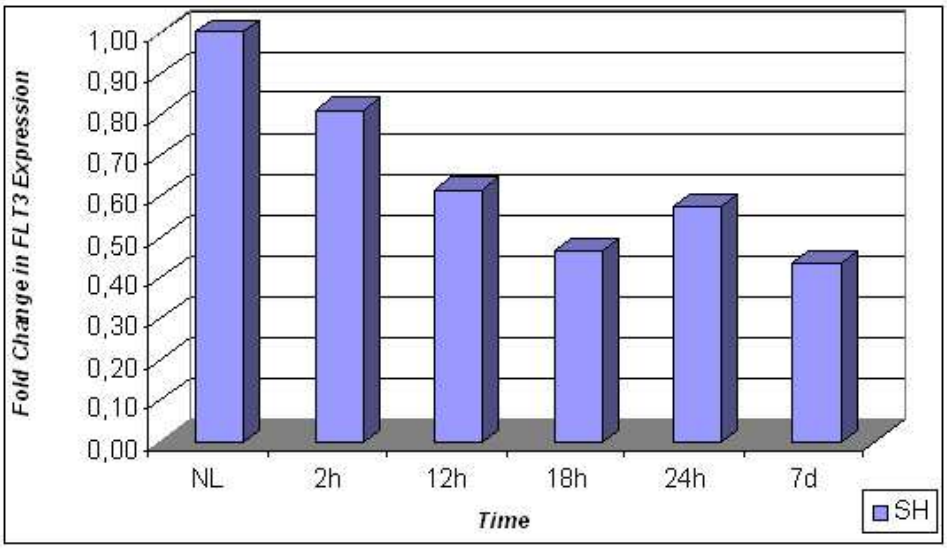

Figure 4.12: *Fold Change in FLT3 expression in SH Groups*

NAME	***FLT3 C_t***	***CYC C_t***	ΔC_t	$2^{-(\Delta C_t - \Delta C_{t_{NL}})}$
NL	22,7	13,3	9,4	1,00
PH 2h	22,5	13,9	8,6	1,74
PH 12h	23,8	13,7	10,1	0,62
PH 18h	26,1	13,9	12,2	0,14
PH 24h	23,7	12,3	11,4	0,25
PH 7d	21,7	12,4	9,3	1,07

Table 4.4: *Real-Time RT-PCR Data For PH Groups*

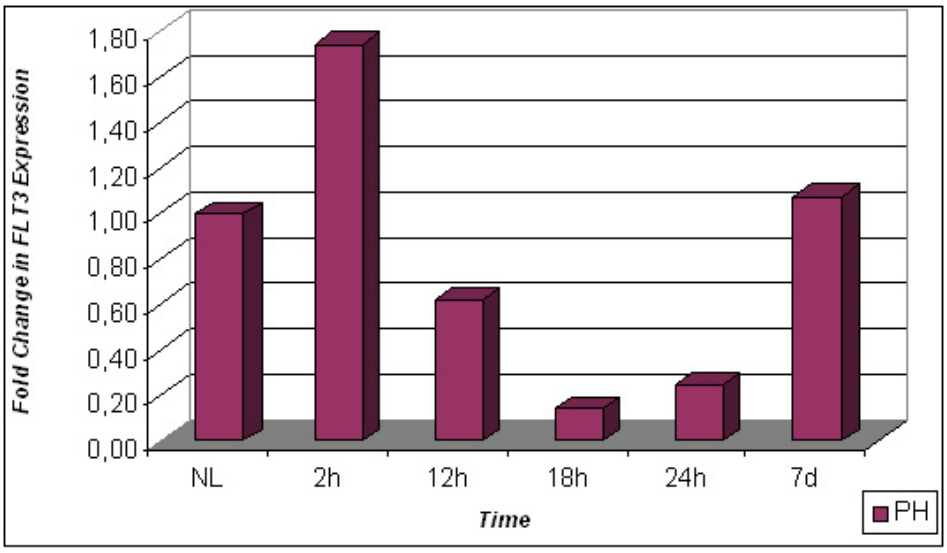

Figure 4.13: *Fold Change in FLT3 expression in PH Groups*

4.4.2 Expression of FLT3 in AAF-Treated SH and PH Groups

The C_t values of AAF-treated SH and PH groups (normal liver, 0 hour, 2 hours, 12 hours, 18 hours, 24 hours and 7 days) for both *FLT3* and *CYC* were collected. The C_t values of the AAF-treated PH groups were normalized according to the difference between the C_t values of normal liver samples and 0 hour samples in both groups. By using normalized C_t values, ΔC_t ($\Delta C_{t_{FLT3}} - \Delta C_{t_{CYC}}$) value for each group is calculated. Fold change in expression of *FLT3* was calculated by using $2^{-(\Delta C_t - \Delta C_{t_{NL}})}$ formula. For calculation, ΔC_t of normal liver sample was used as calibrator. Table 4.5 and Table 4.6 show the real-time RT-PCR data and the results of the calculations for AAF-treated SH and PH groups, respectively. Figure 4.14 and Figure 4.15 show the fold changes of FLT3 expression graphics for AAF-treated SH and PH groups, respectively.

In AAF-treated SH groups (Figure 4.14), except 24 hours sample, an important change in FLT3 expression was not seen. Real-time RT-PCR results of AAF-treated SH groups were consistent with semi-quantitative RT-PCR results. The correlation value between these groups was 0,95. In AAF-treated PH groups (Figure 4.15), a great decrease in FLT3 expression was seen in all the groups after 2 hours. However, the correlation of semi-quantitative RT-PCR results and real-time RT-PCR results was not as high as previous groups. The correlation for AAF-treated PH groups was 0,45.

NAME	***FLT3 C_t***	***CYC C_t***	ΔC_t	$2^{-(\Delta C_t - \Delta C_{t_{NL}})}$
NL	23,5	16,1	7,4	1,00
AAF 0h	22,6	15,5	7,1	1,23
SH-AAF 2h	23,3	15,2	8,1	0,62
SH-AAF 12h	22,5	15,0	7,5	0,93
SH-AAF 18h	22,4	14,8	7,6	0,90
SH-AAF 24h	24,8	14,9	10,0	0,17
SH-AAF 7d	22,8	15,1	7,7	0,81

Table 4.5: *Real-Time RT-PCR Data For AAF-Treated SH Groups*

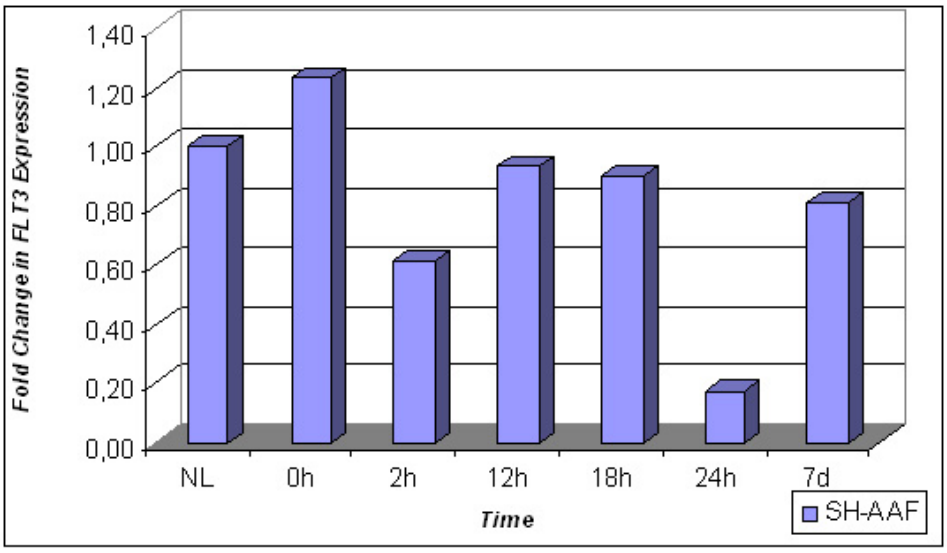

Figure 4.14: *Fold Change in FLT3 expression in AAF-Treated SH Groups*

NAME	***FLT3 C_t***	***CYC C_t***	ΔC_t	$2^{-(\Delta C_t - \Delta C_{t_{NL}})}$
NL	23,6	16,4	7,2	1,00
AAF 0h	22,5	15,2	7,3	0,97
PH-AAF 2h	23,9	15,1	8,8	0,34
PH-AAF 12h	23,6	14,3	9,3	0,23
PH-AAF 18h	23,0	14,1	8,8	0,33
PH-AAF 24h	23,4	14,2	9,1	0,27
PH-AAF 7d	23,0	14,5	8,5	0,42

Table 4.6: *Real-Time RT-PCR Data For AAF-Treated PH Groups*

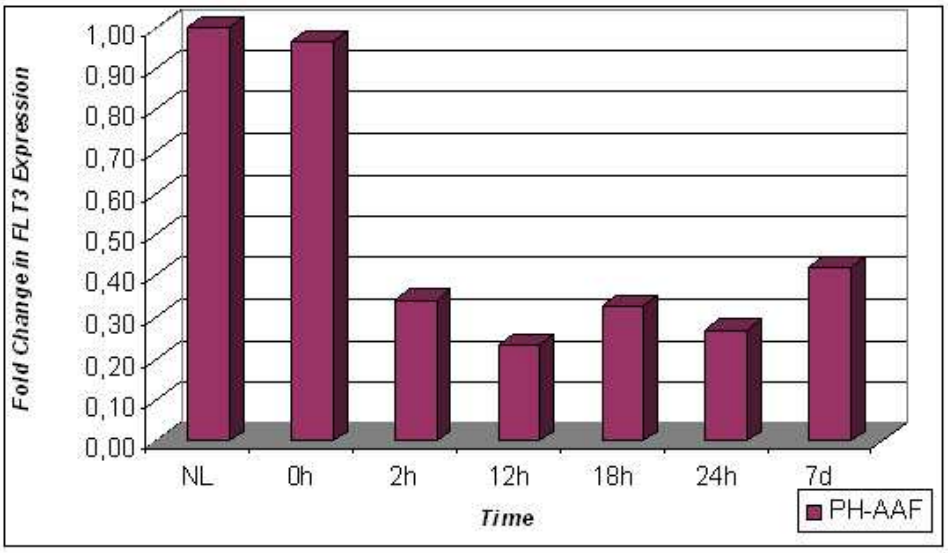

Figure 4.15: *Fold Change in FLT3 expression in AAF-Treated PH Groups*

4.5 Western Blotting Results

4.5.1 Western Blotting of SH and PH Groups

Protein isolation and Western blotting were performed as explained in Section 3.8 and 3.9. The proteins extracted from SH and PH groups were subjected to Western Blotting with anti-FLT3 antibody. As equal loading control, the proteins were run on SDS-PAGE and the gel was stained with Coomassie Brilliant Blue.

FLT3 protein level was similar in all SH groups. However, in PH groups, FLT3 protein started to increase after 48 hours past operation. (Figure 4.16A).

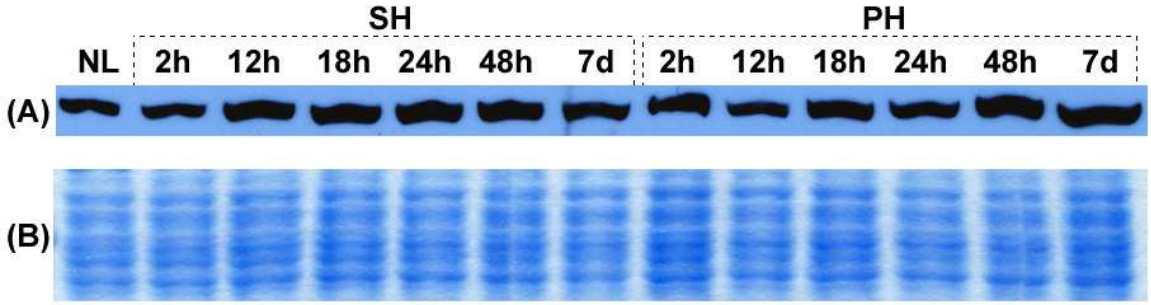

Figure 4.16: *Western Blotting of SH and PH Groups. (A) Western blotting of different proteins extracted from SH and PH groups with anti-FLT3 antibody and (B) Coomassie staining of SDS-PAGE of same proteins.*

4.5.2 Western Blotting of AAF-Treated SH and PH Groups

Protein isolation and Western blotting were performed as explained in Section 3.8 and 3.9. The proteins extracted from AAF-treated SH and PH groups were subjected to Western Blotting with anti-FLT3 antibody. As equal loading control,

the proteins were run on SDS-PAGE and the gel was stained with Coomassie Brilliant Blue.

In AAF-treated SH groups, an increase at protein level was observed in 18^{th} hour and 24^{th} hour. In AAF-treated PH groups, a decrease at protein level was observed from 18^{th} hour through 7^{th} day (Figure 4.17A).

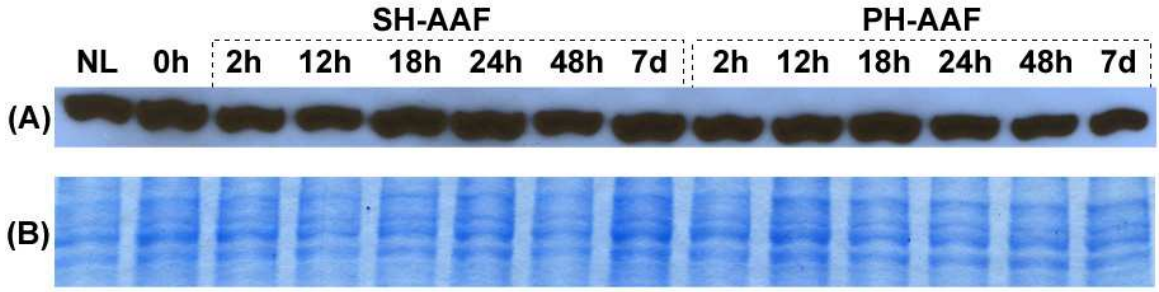

Figure 4.17: *Western Blotting of AAF-Treated SH and PH Groups. (A) Western blotting of different proteins extracted from AAF-treated SH and PH groups with anti-FLT3 antibody and (B) Coomassie staining of SDS-PAGE of same proteins.*

4.6 Immunohistochemistry

In Western blotting studies, we observed FLT3 protein in all samples. In order to examine the location of FLT3 in these groups we performed immunoperoxidase assay on normal liver (NL) and AAF-treated SH and PH groups. IHC is performed as described in Section 3.10.

We first examined the presence of FLT3 protein in NL (Figure 4.18A), and AAF-treated liver (Figure 4.18C), and found its expression in both samples. The negative control (Figure 4.18B) did not reveal any staining.

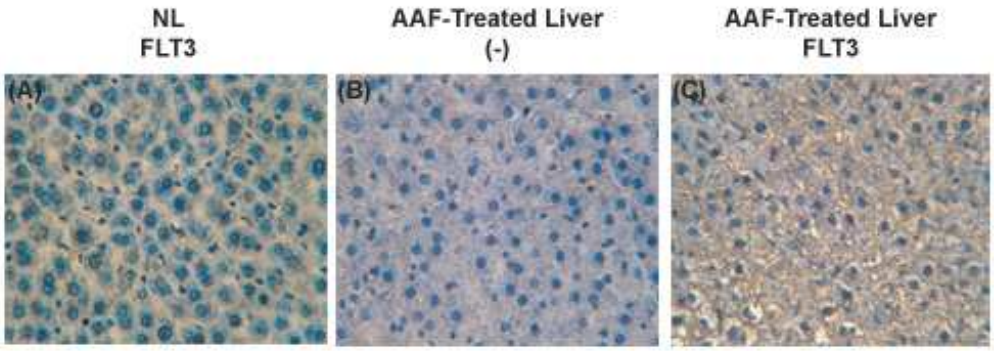

Figure 4.18: *Immunohistochemistry of Normal Liver and AAF-Treated Liver. (A) is IHC of NL with anti-FLT3 antibody, (B) is negative control of IHC of AAF-treated liver, and (C) is IHC of AAF-treated liver with anti-FLT3 antibody.*

Then we performed IHC to all our PH and SH groups (Figure 4.19). Similar to normal liver, we found the expression of FLT3 in those groups. Interestingly the cellular localization of this protein was different among our samples. In all AAF-treated SH groups and early PH groups (2 hours, 12 hours, and 18 hours), FLT3 was located on plasma membrane. But in late PH groups (24 hours and 7 days) FLT3 was mainly seen in the cytoplasm (Figure 4.20).

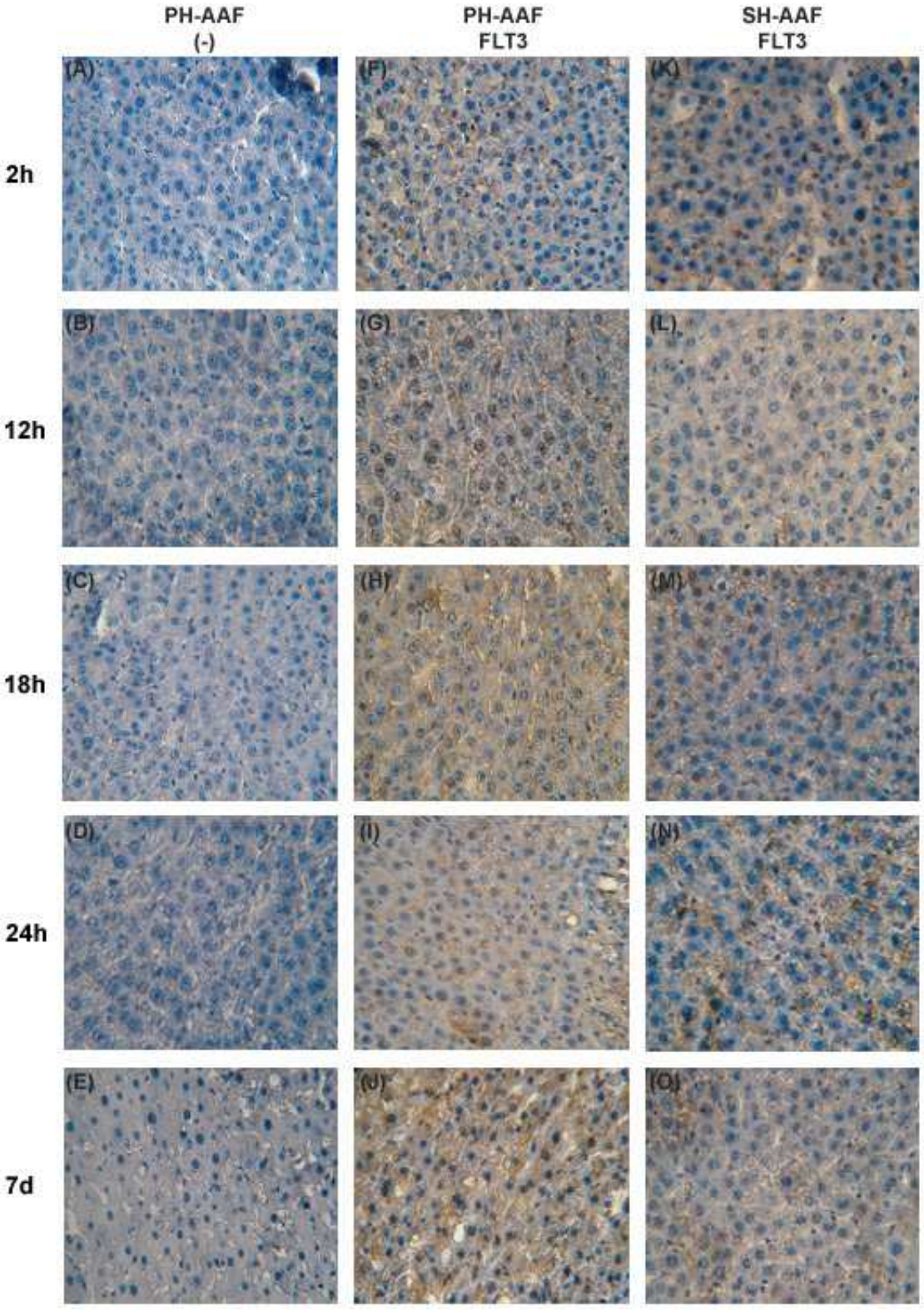

Figure 4.19: *Immunohistochemistry of AAF-Treated SH and PH Groups. (A)-(E) negative controls of PH groups, (F)-(J) IHC of PH groups, and (K)-(O) IHC of SH groups.*

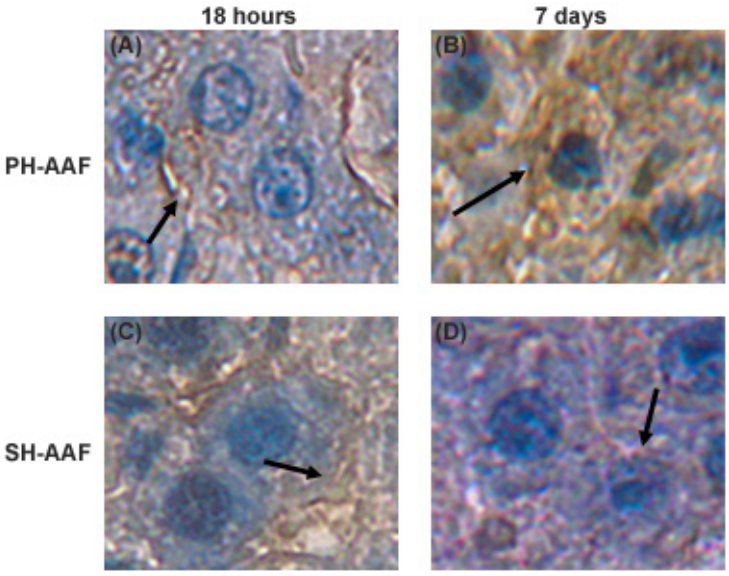

Figure 4.20: *Comparison of IHC Results of 18 hours and 7 days Groups. The location of FLT3 protein is shown with black arrows.*

Chapter 5

Discussion

5.1 Discussion

Liver regeneration, first mentioned in legend of Prometheus, is a complex physiological response that takes place after the loss of hepatocytes caused by toxic or viral injury or secondary liver resection. During regeneration, series of reactions take place to survive the organism, and proliferative and apoptotic mechanisms operate to provide a balance for the survival. Previously, our lab has shown the involvement of *bcl-2* family of genes during liver regeneration (Akcali *et al*, 2004). Therefore, in this study we focused on the other aspect of liver regeneration; mechanisms or participants of the proliferative response.

Recent data revealed that hepatocytes can regenerate or proliferate from three types of cells. After normal liver tissue renewal or if the liver damage is less severe, mature hepatocytes respond rapidly to liver injury. On the other hand, in response to allyl alcohol injury or during hepatocarcinogenesis, exogenous liver stem cells, which may derive from circulating HSCs or bone marrow stem cells take part. These are multipotent cells and have very long proliferation potential, but are rare. Finally, oval cells, which are activated to proliferate when the liver damage is extensive and chronic, or if proliferation of hepatocytes is inhibited,

may be the source of new hepatocytes (Zhang *et al*, 2003). Those cells can be regarded as bipotential precursors for the two hepatic parenchymal cell lineages; hepatocytes or cholangiocytes (Sirica, 1995). Canal of Hering is known as the source of precursors of oval cells. In addition, Hong *et al* (2005) very recently showed that bone marrow-derived mesenchymal stem cells have the potential to differentiate into hepatocyte-like cells passing through oval cell stage. This study strongly suggests that the progenitors of oval cells may initially come from bone marrow. Oval cells express specific proteins and FLT3 is considered as one of these proteins. Therefore, Hong *et al*'s data may explain the reason of existence of a hematopoietic stem cell marker, FLT3, in oval cells; since they share common progenitors.

FLT3 is a subclass III RTK, which is a well-known hematopoietic stem cell marker as well as a hepatic lineage surface marker as well (Hong *et al*, 2005). Therefore, its existence in oval cells supports its role in hepatocyte development. Being a RTK it is logical for FLT3 to assign a role during liver regeneration. However, its expression pattern is not known during liver regeneration. Therefore, we aimed to investigate the expression profile of FLT3 during different models of rat liver regeneration.

The first model we used, was regeneration after partial hepatectomy. The second model was progenitor cell-dependent liver regeneration which was triggered with AAF-treatment in combination with PH.

In both models, there was a reduction at mRNA transcript level of FLT3 after PH (Figures 4.9, 4.11, 4.13, 4.15). In SH groups, the anesthetic we used may have an effect on the expression profile of liver cells, that may be the reason of the differences in the FLT3 level in SH groups. The reduction of mRNA transcript level of FLT3 in PH groups may be related with the massive loss of cells. Except late AAF-treated PH groups, we did not observe a correlation between Western blotting results and RT-PCR result which suggests that, transcriptional regulation of FLT3 does not take place during regeneration. Therefore, we focused on the translational events. When we examined the data regarding the amount of

FLT3 protein only in the late stages of AAF-treated PH groups there was a correlation between FLT3 protein level and transcript level. Apart from these groups the protein level was almost equal in all other groups. In order to draw exact conclusions from RT-PCR and Western blotting data, the experiments should be repeated and statistical calculations should be done.

On the other hand, our immunohistochemistry studies revealed a different pattern in the localization of FLT3 protein in different experimental groups (Figure 4.20). In all AAF-treated SH groups and in early groups of AAF-treated PH samples (2 hours, 12 hours and 18 hours), FLT3 expression was seen exclusively on the plasma membrane. Whereas, in later AAF-treated PH groups, especially in 7 days after PH group, there was a strong cytoplasmic staining.

The data regarding to the cellular difference in the expression of FLT3 during early and late stages of liver regeneration strongly suggests the activation status of the receptor. Under normal conditions (normal liver and SH groups), FLT3 resides in the plasma membrane in inactive monomeric form. When liver injury occurs, the liver undergoes a regeneration process and during this process FLT3 can be activated in order to relay signals for proliferative events. This activation is followed by internalization of receptors as shown by Turner *et al* (1996) and ultimately results in degradation. Therefore, the cytoplasmic staining of FLT3 protein that we observed in late AAF-treated PH groups may be the internalized FLT3 receptors. This data suggests that, FLT3 is activated during this regenerative process. Also, Western blotting results of 24 hours and 7 days groups of AAF-treated PH groups support the model in which FLT3 is activated at late regenerative stages. In these Western blots, we saw a decrease at FLT3 protein in 24 hours and 7 days samples which may be explained with degradation of FLT3 receptor.

When all our findings are gathered, a likely scenario would be as follows; under normal conditions FLT3 is expressed at a constant level in liver, and it is located in the plasma membrane in monomeric inactive form. In SH groups, since liver regeneration is not triggered, FLT3 is seen in membrane bound inactive monomeric form. The situation is also the same in early PH groups. In late PH

groups, FLT3 is activated upon ligand binding and dimerization, in order to initiate several intercellular signal transduction mechanisms which leads to cell proliferation. Then the activated FLT3 receptors rapidly undergo internalization and degradation, therefore FLT3 is seen in the cytoplasm in PH groups.

5.2 Future Perspective

Our studies reveals preliminary data, that FLT3 is activated during progenitor-cell dependent liver regeneration. For understanding the exact role of FLT3 in this process further studies should be performed.

A protein kinase assay would provide significant data about activity of FLT3 in regeneration. Besides, kinase activity assays, other studies can provide valuable data.

In order to confirm that cytoplasmic FLT3 staining in late AAF-treated PH groups indicate internalization of the activated receptor, further studies should be performed. Cytoplasmic proteins and membrane bound proteins can be isolated separately and Western blotting can be performed on these protein samples to investigate if FLT3 is actually seen in cytoplasm in late PH groups. Besides, Western studies with anti-FLT3 antibody that recognizes only the phosphorylated form of the receptor should be performed.

It is important to see if overexpression of FLT3 would affect liver regeneration. Some studies showed that, when a plasmid carrying a gene is injected to the tail vein of rat, the expression of the gene of interest is seen in liver 24 hours after injection (Lui and Huang 2002; Maruyama *et al*, 2004). By using this method FLT3 overexpression can be maintained in liver and whether overexpression of FLT3 has an effect on liver regeneration can be examined.

Also, FLT3 expression can be blocked by using RNA interference technology and its effects on liver regeneration can be observed. For achieving silencing, the tail vein injection protocol can be adapted to this method.

In addition to studies on FLT3 receptor, investigating the expression profile of FLT3 ligand may provide data about FLT3 activity during liver regeneration.

Chapter 6

References

Agnes, F., Shamoon, B., Dina, C., Rosnet, O., Birnbaum, D., and Galibert, F. (1994). Genomic structure of the downstream part of the human FLT3 gene: exon/intron structure conservation among genes encoding receptor tyrosine kinases (RTK) of subclass III. *Gene.* 145(2):283-288.

Akcali, K. C., Dalgic, A., Ucar, A., Haj, K. B., and Guvenc, D. (2004). Expression of bcl-2 gene family during resection induced liver regeneration: comparison between hepatectomized and sham groups. *World J Gastroenterol.* 10(2):279-283.

Alison, M., Golding, M., Lalani, el, and Sarraf, C. (1998). Wound healing in the liver with particular reference to stem cells. *Philos.Trans.R.Soc.Lond B Biol Sci.* 353(1370):877-894.

Arber, N., Zajicek, G., and Ariel, I. (1988). The streaming liver. II. Hepatocyte life history. *Liver.* 8(2):80-87.

Baumann, U., Crosby, H. A., Ramani, P., Kelly, D. A., and Strain, A. J. (1999). Expression of the stem cell factor receptor c-kit in normal and diseased pediatric liver: identification of a human hepatic progenitor cell? *Hepatology.* 30(1):112-117.

Bottaro, D. P., Rubin, J. S., Faletto, D. L., Chan, A. M., Kmiecik, T. E., Vande Woude, G. F., and Aaronson, S. A. (1991). Identification of the hepatocyte growth factor receptor as the c-met proto-oncogene product. *Science*. 251(4995):802-804.

Bralet, M. P., Branchereau, S., Brechot, C., and Ferry, N. (1994). Cell lineage study in the liver using retroviral mediated gene transfer. Evidence against the streaming of hepatocytes in normal liver. *Am.J Pathol*. 144(5):896-905.

Bucher, N. L. and Swaffield, M. N. (1964). The rate of incorporation of labeled thymidine into the deoxyribonucleic acid of regenerating rat liver in relation to the amount of liver excised. *Cancer Res*. 24:1611-1625.

Carola, R., Harley, J. P., and Noback, C. R. (1992). Human Anatomy. McGraw-Hill Inc, USA.

Cressman, D. E., Greenbaum, L. E., DeAngelis, R. A., Ciliberto, G., Furth, E. E., Poli, V., and Taub, R. (1996). Liver failure and defective hepatocyte regeneration in interleukin-6-deficient mice. *Science*. 274(5291):1379-1383.

Cruise, J. L., Houck, K. A., and Michalopoulos, G. (1988). Early events in the regulation of hepatocyte DNA synthesis: the role of alpha-adrenergic stimulation. *Scand.J Gastroenterol.Suppl*. 15119-30.

Cruise, J. L. (1991). Alpha 1-adrenergic receptors in liver regeneration. *Dig.Dis.Sci*. 36(4):485-488.

Evarts, R. P., Nakatsukasa, H., Marsden, E. R., Hsia, C. C., Dunsford, H. A., and Thorgeirsson, S. S. (1990). Cellular and molecular changes in the early stages of chemical hepatocarcinogenesis in the rat. *Cancer Res*. 50(11):3439-3444.

Fausto, N., Lemire, J. M., and Shiojiri, N. (1993). Cell lineages in hepatic development and the identification of progenitor cells in normal and injured liver. *Proc.Soc.Exp.Biol.Med*. 204(3):237-241.

Fausto, N., Laird, A. D., and Webber, E. M. (1995). Role of growth factors and cytokines in hepatic regeneration. *FASEB J.* 9(15):1527-1536.

Fausto, N. (2001). Liver regeneration: from laboratory to clinic. *Liver Transpl.* 7(10):835-844.

Fausto, N. and Campbell, J. S. (2003). The role of hepatocytes and oval cells in liver regeneration and repopulation. *Mech.Dev.* 120(1):117-130.

Fujio, K., Evarts, R. P., Hu, Z., Marsden, E. R., and Thorgeirsson, S. S. (1994). Expression of stem cell factor and its receptor, c-kit, during liver regeneration from putative stem cells in adult rat. *Lab Invest.* 70(4):511-516.

Gilbert, S. F. (2003). Developmental Biology. Sinauer Associates Inc, USA.

Gordon, G. J., Coleman, W. B., Hixson, D. C., and Grisham, J. W. (2000). Liver regeneration in rats with retrorsine-induced hepatocellular injury proceeds through a novel cellular response. *Am.J Pathol.* 156(2):607-619.

Grompe, M. and Finegold, M. J. (2001). Liver Stem Cells. In Marshak, D. R., Gardner, R. L, and Gottlieb, D. Stem Cell Biology. Cold Spring Harbor Laboratory Press, USA.

Grompe, M. (2004). Adult Liver Stem Cells. In Lanza, R., Blau, H., Melton, D., Moore, M., Thomas, E. D., Adam, R., Verfaillie, C., Weissman, I., and West, M. Handbook of Stem Cells (Volume 2). Elsevier Academic Press, USA.

Guyton, A. C. and Hall, J. E. (1997). Text Book of Medical Physiology. W.B. Saunders Company, USA.

Higgins, M. and Anderson, R. M. (1931). Experimental pathology of the liver. I. Restoration of the liver of the white rat following partial surgical removal. *Arch.Pathol.* 12186-202.

Hong, S. H., Gang, E. J., Jeong, J. A., Ahn, C., Hwang, S. H., Yang, I. H., Park, H. K., Han, H., and Kim, H. (2005). In vitro differentiation of human umbilical cord blood-derived mesenchymal stem cells into hepatocyte-like cells. *Biochem.Biophys.Res Commun.* 330(4):1153-1161.

Jirtle, R. L., Carr, B. I., and Scott, C. D. (1991). Modulation of insulin-like growth factor-II/mannose 6-phosphate receptors and transforming growth factor-beta 1 during liver regeneration. *J Biol.Chem.* 266(33):22444-22450.

Katayama, S., Tateno, C., Asahara, T., and Yoshizato, K. (2001). Size-dependent in vivo growth potential of adult rat hepatocytes. *Am.J Pathol.* 158(1):97-105.

Kennedy, S., Rettinger, S., Flye, M. W., and Ponder, K. P. (1995). Experiments in transgenic mice show that hepatocytes are the source for postnatal liver growth and do not stream. *Hepatology.* 22(1):160-168.

Koniaris, L. G., McKillop, I. H., Schwartz, S. I., and Zimmers, T. A. (2003). Liver regeneration. *J.Am.Coll.Surg.* 197(4):634-659.

Kountouras, J., Boura, P., and Lygidakis, N. J. (2001). Liver regeneration after hepatectomy. *Hepatogastroenterology.* 48(38):556-562.

Kruglov, E. A., Jain, D., and Dranoff, J. A. (2002). Isolation of primary rat liver fibroblasts. *J Investig.Med.* 50(3):179-184.

Laconi, E., Sarma, D. S., and Pani, P. (1995). Transplantation of normal hepatocytes modulates the development of chronic liver lesions induced by a pyrrolizidine alkaloid, lasiocarpine. *Carcinogenesis.* 16(1):139-142.

Laconi, E., Oren, R., Mukhopadhyay, D. K., Hurston, E., Laconi, S., Pani, P., Dabeva, M. D., and Shafritz, D. A. (1998). Long-term, near-total liver replacement by transplantation of isolated hepatocytes in rats treated with retrorsine. *Am.J Pathol.* 153(1):319-329.

Lemire, J. M., Shiojiri, N., and Fausto, N. (1991). Oval cell proliferation and the origin of small hepatocytes in liver injury induced by D-galactosamine. *Am.J Pathol.* 139(3):535-552.

Lemmer, E. R., Shepard, E. G., Blakolmer, K., Kirsch, R. E., and Robson, S. C. (1998). Isolation from human fetal liver of cells co-expressing CD34 haematopoietic stem cell and CAM 5.2 pancytokeratin markers. *J Hepatol.* 29(3):450-454.

Lindroos, P. M., Zarnegar, R., and Michalopoulos, G. K. (1991). Hepatocyte growth factor (hepatopoietin A) rapidly increases in plasma before DNA synthesis and liver regeneration stimulated by partial hepatectomy and carbon tetrachloride administration. *Hepatology.* 13(4):743-750.

Liu, F. and Huang, L. (2002). Noninvasive gene delivery to the liver by mechanical massage. *Hepatology.* 35(6):1314-1319.

Livak, K. J. and Schmittgen, T. D. (2001). Analysis of relative gene expression data using real-time quantitative PCR and the $2^{-\Delta\Delta C_t}$ Method. *Methods.* 25(4):402-408.

Markovic, A., MacKenzie, K. L., and Lock, R. B. (2005). FLT-3: a new focus in the understanding of acute leukemia. *Int.J Biochem.Cell Biol.* 37(6):1168-1172.

Maruyama, H., Higuchi, N., Kameda, S., Miyazaki, J., and Gejyo, F. (2004). Rat liver-targeted naked plasmid DNA transfer by tail vein injection. *Mol.Biotechnol.* 26(2):165-172.

Matthews, W., Jordan, C. T., Wiegand, G. W., Pardoll, D., and Lemischka, I. R. (1991). A receptor tyrosine kinase specific to hematopoietic stem and progenitor cell-enriched populations. *Cell.* 65(7):1143-1152.

Mead, J. E. and Fausto, N. (1989). Transforming growth factor alpha may be a physiological regulator of liver regeneration by means of an autocrine mechanism. *Proc.Natl.Acad.Sci.U.S.A.* 86(5):1558-1562.

Michalopoulos, G., Houck, K. A., Dolan, M. L., and Leutteke, N. C. (1984). Control of hepatocyte replication by two serum factors. *Cancer Res.* 44(10):4414-4419.

Michalopoulos, G. K. and DeFrances, M. C. (1997). Liver regeneration. *Science.* 276(5309):60-66.

Mitaka, T. (2001). Hepatic stem cells: from bone marrow cells to hepatocytes. *Biochem.Biophys.Res Commun.* 281(1):1-5.

Noguchi, S., Ohba, Y., and Oka, T. (1991). Influence of epidermal growth factor on liver regeneration after partial hepatectomy in mice. *J Endocrinol.* 128(3):425-431.

Omori, N., Omori, M., Evarts, R. P., Teramoto, T., Miller, M. J., Hoang, T. N., and Thorgeirsson, S. S. (1997). Partial cloning of rat CD34 cDNA and expression during stem cell-dependent liver regeneration in the adult rat. *Hepatology.* 26(3):720-727.

Overturf, K., al-Dhalimy, M., Ou, C. N., Finegold, M., and Grompe, M. (1997). Serial transplantation reveals the stem-cell-like regenerative potential of adult mouse hepatocytes. *Am.J Pathol.* 151(5):1273-1280.

Paul, J., Conkie, D., and Freshney, R. I. (1969). Erythropoietic cell population changes during the hepatic phase of erthropoiesis in the fetal mouse. *Cell Tissue Kinet.* 2:283-294.

Petersen, B. E., Goff, J. P., Greenberger, J. S., and Michalopoulos, G. K. (1997). Hepatic oval cells express the haematopoietic stem cell marker Thy-1 in the rat. *Hepatology.* 27433-445.

Petersen, B. E., Bowen, W. C., Patrene, K. D., Mars, W. M., Sullivan, A. K., Murase, N., Boggs, S. S., Greenberger, J. S., and Goff, J. P. (1999). Bone marrow as a potential source of hepatic oval cells. *Science.* 284(5417):1168-1170.

Ponder, K. P. (1996). Analysis of liver development, regeneration, and carcinogenesis by genetic marking studies. *FASEB J.* 10(7):673-682.

Rosnet, O., Marchetto, S., deLapeyriere, O., and Birnbaum, D. (1991). Murine Flt3, a gene encoding a novel tyrosine kinase receptor of the PDGFR/CSF1R family. *Oncogene.* 6(9):1641-1650.

Rosnet, O., Schiff, C., Pebusque, M. J., Marchetto, S., Tonnelle, C., Toiron, Y., Birg, F., and Birnbaum, D. (1993). Human FLT3/FLK2 gene: cDNA cloning and expression in hematopoietic cells. *Blood.* 82(4):1110-1119.

Ross, M. H., Reith, E. J., and Romrell, L. J. (1989). Histology: A Text and Atlas. Williams and Wilkins, USA.

Schwarze, P. E., Pettersen, E. O., Shoaib, M. C., and Seglen, P. O. (1984). Emergence of a population of small, diploid hepatocytes during hepatocarcinogenesis. *Carcinogenesis.* 5(10):1267-1275.

Shinozuka, H., Lombardi, B., Sell, S., and Iammarino, R. M. (1978). Early histological and functional alterations of ethionine liver carcinogenesis in rats fed a choline-deficient diet. *Cancer Res.* 38(4):1092-1098.

Shiojiri, N., Imai, H., Goto, S., Ohta, T., Ogawa, K., and Mori, M. (1997). Mosaic pattern of ornithine transcarbamylase expression in spfash mouse liver. *Am.J Pathol.* 151(2):413-421.

Shiojiri, N., Sano, M., Inujima, S., Nitou, M., Kanazawa, M., and Mori, M. (2000). Quantitative analysis of cell allocation during liver development, using the spf^{ash}-heterozygous female mouse. *Am.J Pathol.* 156(1):65-75.

Short, J., Klein, K., Kibert, L., and Ove, P. (1980). Involvement of the lodothyronines in liver and hepatoma cell proliferation in the rat. *Cancer Res.* 40(7):2417-2422.

Simpkins, J. and Williams, J. I. (1998). Advanced Human Biology. Collins Educational, Milan.

Sirica, A. E., Mathis, G. A., Sano, N., and Elmore, L. W. (1990). Isolation, culture, and transplantation of intrahepatic biliary epithelial cells and oval cells. *Pathobiology.* 58(1):44-64.

Sirica, A. E. (1995). Ductular hepatocytes. *Histol.Histopathol.* 10(2):433-456.

Solt, D. B., Medline, A., and Farber, E. (1977). Rapid emergence of carcinogen-induced hyperplastic lesions in a new model for the sequential analysis of liver carcinogenesis. *Am.J Pathol.* 88(3):595-618.

Stirewalt, D. L. and Radich, J. P. (2003). The role of FLT3 in haematopoietic malignancies. *Nat.Rev.Cancer.* 3(9):650-665.

Strain, A. J. and Crosby, H. A. (2000). Hepatic stem cells. *Gut.* 46(6):743-745.

Taub, R. (1996). Liver regeneration 4: transcriptional control of liver regeneration. *FASEB J.* 10(4):413-427.

Teebor, G. W. and Becker, F. F. (1971). Regression and persistence of hyperplastic hepatic nodules induced by N-2-Fluorenylacetamide and their relationship to hepatocarcinogenesis. *Cancer Res.* 31(1):1-3.

Theise, N. D., Saxena, R., Portmann, B. C., Thung, S. N., Yee, H., Chiriboga, L., Kumar, A., and Crawford, J. M. (1999). The canals of Hering and hepatic stem cells in humans. *Hepatology.* 30(6):1425-1433.

Theise, N. D., Badve, S., Saxena, R., Henegariu, O., Sell, S., Crawford, J. M., and Krause, D. S. (2000). Derivation of hepatocytes from bone marrow cells in mice after radiation-induced myeloablation. *Hepatology.* 31(1):235-240.

Thurman, R. G. and Kauffman, F. C. (1985). Sublobular compartmentation of pharmacologic events (SCOPE): metabolic fluxes in periportal and pericentral regions of the liver lobule. *Hepatology.* 5(1):144-151.

Timchenko, N. A., Wilde, M., Nakanishi, M., Smith, J. R., and Darlington, G. J. (1996). CCAAT/enhancer-binding protein alpha (C/EBP alpha) inhibits cell proliferation through the p21 (WAF-1/CIP-1/SDI-1) protein. *Genes Dev.* 10(7):804-815.

Turner, A. M., Lin, N. L., Issarachai, S., Lyman, S. D., and Broudy, V. C. (1996). FLT3 receptor expression on the surface of normal and malignant human hematopoietic cells. *Blood.* 88(9):3383-3390.

Vessey, C. J. and de la Hall, P. M. (2001). Hepatic stem cells: a review. *Pathology.* 33(2):130-141.

Wang, N. D., Finegold, M. J., Bradley, A., Ou, C. N., Abdelsayed, S. V., Wilde, M. D., Taylor, L. R., Wilson, D. R., and Darlington, G. J. (1995). Impaired energy homeostasis in C/EBP alpha knockout mice. *Science.* 269(5227):1108-1112.

Weiss, A. and Schlessinger, J. (1998). Switching signals on or off by receptor dimerization. *Cell.* 94(3):277-280.

Wu, H., Wade, M., Krall, L., Grisham, J., Xiong, Y., and Van, Dyke T. (1996). Targeted in vivo expression of the cyclin-dependent kinase inhibitor p21 halts hepatocyte cell-cycle progression, postnatal liver development and regeneration. *Genes Dev.* 10(3):245-260.

Yamada, Y., Kirillova, I., Peschon, J. J., and Fausto, N. (1997). Initiation of liver growth by tumor necrosis factor: deficient liver regeneration in mice lacking type I tumor necrosis factor receptor. *Proc.Natl.Acad.Sci.U.S.A.* 94(4):1441-1446.

Yamada, Y. and Fausto, N. (1998). Deficient liver regeneration after carbon tetrachloride injury in mice lacking type 1 but not type 2 tumor necrosis factor receptor. *Am.J Pathol.* 152(6):1577-1589.

Yin, L., Ghebranious, N., Chakraborty, S., Sheehan, C. E., Ilic, Z., and Sell, S. (1998). Control of mouse hepatocyte proliferation and ploidy by p53 and p53ser246 mutation in vivo. *Hepatology.* 27(1):73-80.

Zajicek, G., Oren, R., and Weinreb, M., Jr. (1985). The streaming liver. *Liver*. 5(6):293-300.

Zaret, K. S. (2000). Liver specification and early morphogenesis. *Mech.Dev.* 92(1):83-88.

Zhang, Y., Bai, X. F., and Huang, C. X. (2003). Hepatic stem cells: existence and origin. *World J Gastroenterol*. 9(2):201-204.